STUDY OF THE EFFECT OF NIP DIAMETER UPON THE RATE OF NIP INDUCED TENSION

By

MOHAN PRABHAKAR

Bachelor of Engineering

Mysore University

Mysore, India

1983

Submitted to the Faculty of the
Graduate College of the
Oklahoma State University
in partial fulfillment of
the requirements for
the degree of
MASTER OF SCIENCE
May, 1994

OKLAHOMA STATE UNIVERSITY

STUDY OF THE EFFECT OF NIP DIAMETER

UPON THE RATE OF NIP INDUCED

TENSION

Thesis Approved:

Thesis Adviser

Dean of the Graduate College

ACKNOWLEDGMENT

I wish to express my sincere appreciation to my graduate advisor, Dr.J.K.Good, for his constructive guidance, intelligent supervision and moral support during my graduate study. My sincere appreciation extends to my other committee members Dr.C.E.Price and Dr.J.J.Shelton, whose guidance, assistance, encouragement and friendship are also invaluable.

Moreover, I wish to express my sincere gratitude to Mr. Nandakumar and those who provided suggestions and advice during this study.

This publication is a result of research which was funded by the Web Handling research Center of Oklahoma State University. I would like to thank the sponsors of the WHRC for supporting this research. The sponsors include the National Science Foundation, the Noble Foundation, the State of Oklahoma and an industrial consortium of which Beloit Corporation, Polaroid Corporation, Velmet-Appleton Inc., Fife Corporation, Hoechst-Celanese Corporation, 3M Company, Mobil Chemical Company, E.I.Dupont de Nemours & Co, Inc., ICI Americas, Kimberly-Clark Corporation, Mead Corporation, Westvaco Corporation, James River Graphics, Eastman Kodak Company and Union Camp Corporation are members.

I owe special thanks to my wife, Geetha, for her sacrifices, encouragement and patience during this study. I would also like to thank my parents who have encouraged and inspired my educational endeavors.

TABLE OF CONTENTS

Chapter		Page
I.	INTRODUCTION	1
	Overview	1
	Purpose and Objective	3
	Organization	3
II.	LITERATURE SURVEY	4
	Background History	4
	Experimental Studies	5
	Finite Element Analysis	7
	Summary	9
III.	ANALYTICAL STUDY	10
	Objective	10
	Approach to the problem	10
	Results of analysis	13
IV.	EXPERIMENTAL ANALYSIS	20
	Experimental Study	20
	Results of experiments	22
V.	FINITE ELEMENT ANALYSIS	38
	Modeling Details	38
	Results of Analysis	41
VI.	DISCUSSIONS	50

Chapter Page

VII. CONCLUSIONS AND FUTURE WORK 58

REFERENCES 60

APPENDIX Finite Element (ANSYS) Code for Analysis 61

LIST OF TABLES

Table		Page
I.	Values of C_1 and C_2 from experimental results based on Nip Diameter	36
II.	Values of C_1 and C_2 from experimental results based on Nip Load	37
III.	Finite element analysis results	48
IV.	Comparison of Nip Induced Stress	56

LIST OF FIGURES

Figure		Page
1.	Center winding with Undriven Nip	2
2.	Contact of two cylindrical surfaces	11
3.	Pressure profile on contact surface	12
4.	Estimated Nip induced stress for 1 inch rolling, with 2.8 pli Nip Load	14
5.	Estimated Nip induced stress for 1 inch rolling, with 8.26 pli Nip Load	14
6.	Estimated Nip induced stress for 1 inch rolling, with 11.77 pli Nip Load	15
7.	Estimated Nip induced stress for 1 inch rolling, with 24 pli Nip Load	15
8.	Comparison of estimated Nip Induced stress for 1 inch rolling with different Nip diameters	16
9.	Comparison of estimated Nip Induced stress for 2.8 pli Nip Load	17
10.	Comparison of estimated Nip Induced stress for 8.26 pli Nip Load	17
11.	Comparison of estimated Nip Induced stress for 11.77 pli Nip Load	18
12.	Comparison of estimated Nip Induced stress for 24 pli Nip Load	18
13.	Experimental set-up	21
14.	Nip Induced Stress Vs Rolling distance for 8" Nip, 2.27 pli nip load	23
15.	Nip Induced Stress Vs Rolling distance for 8" Nip, 2.8 pli nip load	24
16.	Nip Induced Stress Vs Rolling distance for 8" Nip, 8.26 pli nip load	25
17.	Nip Induced Stress Vs Rolling distance for 10" Nip, 2.8 pli nip load	26
18.	Nip Induced Stress Vs Rolling distance for 10" Nip, 8.26 pli nip load	27
19.	Nip Induced Stress Vs Rolling distance for 20" Nip, 8.26 pli nip load	28
20.	Nip Induced Stress Vs Rolling distance for 20" Nip, 11.77 pli nip load	29

Figure Page

21. Nip Induced Stress Vs Rolling distance for 20" Nip, 24 pli nip load 30
22. Nip Induced Stress Vs Rolling distance for 30" Nip, 11.77 pli nip load 31
23. Nip Induced Stress Vs Rolling distance for 30" Nip, 24 pli nip load 32
24. Nip Induced Stress Vs Rolling distance for 60" Nip, 24 pli nip load 33
25. Comparison of experimental results for 2.8 pli Nip Load 34
26. Comparison of experimental results for 8.26 pli Nip Load 34
27. Comparison of experimental results for 11.77 pli Nip Load 35
28. Comparison of experimental results for 24 pli Nip Load 35
29. Finite element model 39
30. Load distribution on the Elements 40
31. Strain plot for 8 inch Diameter Nip and 2.8 pli Nip Load 42
32. Strain plot for 10 inch Diameter Nip and 2.8 pli Nip Load 42
33. Strain plot for 8 inch Diameter Nip and 8.26 pli Nip Load 43
34. Strain plot for 10 inch Diameter Nip and 8.26 pli Nip Load 43
35. Strain plot for 20 inch Diameter Nip and 8.26 pli Nip Load 44
36. Strain plot for 20 inch Diameter Nip and 11.77 pli Nip Load 44
37. Strain plot for 30 inch Diameter Nip and 11.77 pli Nip Load 45
38. Strain plot for 4 inch Diameter Nip and 24 pli Nip Load 45
39. Strain plot for 8 inch Diameter Nip and 24 pli Nip Load 46
40. Strain plot for 10 inch Diameter Nip and 24 pli Nip Load 46
41. Strain plot for 20 inch Diameter Nip and 24 pli Nip Load 47
42. Strain plot for 30 inch Diameter Nip and 24 pli Nip Load 47
43. Strain plot for 60 inch Diameter Nip and 24 pli Nip Load 48

Figure		Page
44.	Comparison of experimental and finite element analysis results for 8 inch Diameter Nip and 2.8 pli Nip Load	50
45.	Comparison of experimental and finite element analysis results for 10 inch Diameter Nip and 2.8 pli Nip Load	51
46.	Comparison of experimental and finite element analysis results for 8 inch Diameter Nip and 8.26 pli Nip Load	51
47.	Comparison of experimental and finite element analysis results for 10 inch Diameter Nip and 8.26 pli Nip Load	52
48.	Comparison of experimental and finite element analysis results for 20 inch Diameter Nip and 8.26 pli Nip Load	52
49.	Comparison of experimental and finite element analysis results for 20 inch Diameter Nip and 11.77 pli Nip Load	53
50.	Comparison of experimental and finite element analysis results for 30 inch Diameter Nip and 11.77 pli Nip Load	53
51.	Comparison of experimental and finite element analysis results for 20 inch Diameter Nip and 24 pli Nip Load	54
52.	Comparison of experimental and finite element analysis results for 30 inch Diameter Nip and 24 pli Nip Load	54
53.	Comparison of experimental and finite element analysis results for 60 inch Diameter Nip and 24 pli Nip Load	55
54a.	Comparison of estimated nip induced stress with 24 pli Nip Load for different Nip Diameters.	57
54b.	Effect of nip diameter on roll hardness	57

NOMENCLATURE

b	*Semi contact width (inch)*
P	*Nip load (Lbf)*
l	*Contact length (inch)*
E	*Modulus of elasticity (Psi)*
υ	*Poisson's ratio*
d	*Diameter of roller*
p_x	*Hertzian pressure distribution*
ε_x	*Strain in machine direction (x-direction)*
σ_x	*Stress in machine direction (x-direction) (Psi)*
μ	*Kinetic coefficient of friction*
T	*Nip induced tension (Lbf)*
T_{max}	*Maximum nip induced tension (Lbf)*
p_{max}	*Maximum Hertzian contact pressure*
x	*Rolling Distance*
h	*Web caliper (inch)*

CHAPTER I

INTRODUCTION

Overview

A web is a continuous, flexible strip of material such as paper, metal foil, plastic film, textiles and non-woven materials which are stored at least on an intermediate basis in wound rolls to accommodate high speed, automated manufacturing operations. Web handling is the science involving the mechanics and dynamics of transporting webs from unwind stations, through process machinery, to rewind stations.

Winding is an integral operation in almost every web handling process. During the course of a web becoming a final product it may be unwound and rewound several times depending upon the number of web process which must be performed. Winding exerts stresses upon webs which often can degrade the quality but it may be seen that the wound roll form is the most efficient and opportune storage format for high speed automated manufacturing processes. It is desirable to control the winding tension of a wound roll to get a stable roll that is free from defects which can result from too little or too much stress being wound into the roll.

Much of the winding which is currently performed is accomplished via a technique which is known as center winding with an undriven nip roll (Fig. 1). This technique requires that the winding torque be provided to the core of the winding roll. An undriven nip roll follows the outside radius of the winding roll. One purpose of the nip is to help exude wound-in air from the wound roll which could lead to an unstable, loosely wound roll package which is apt to sustain web defects during web storage or transport. The second purpose is to provide an increased tension in the web, above the web line tension, for the winding process.

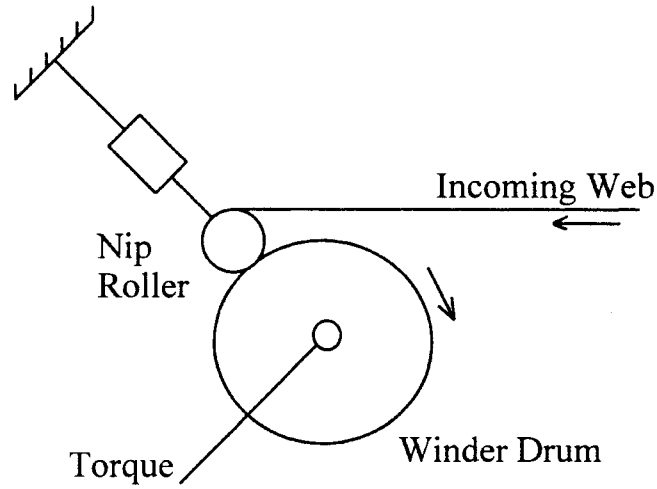

Fig. 1 Center Winder with Undriven Nip

Earlier studies on nip mechanics have indicated that the nip induced tension mainly depends on nip load, nip diameter, winder roll diameter and traction [1,2,4,7,and 8]. It was also discovered that the nip induced tension increased at a higher rate with respect to nip rolling distance when smaller diameter nips were used. In this study an attempt will be made to study the effect of nip diameter on the rate of nip induced tension.

Purpose and Objective

The objectives for this study are :

1. Study the effect of nip diameters on the rate of nip induced stress.
2. Generate a theoretical expression for the wound-in-tension, which is affected by both wound roll and nip radii.
3. Model and analyze the problem using finite element methods.
4. Wind and instrument rolls in lab with large diameter nips.

Initially, an analytical study will be made to estimate the effect of nip diameter on the rate of nip induced tension. This will be followed by the experimental studies and finite element analysis. The outcome of all these will be compared for verification.

Organization

A literature survey is compiled and is presented in Chapter II in which topics concerning the nip diameter effect on the nip induced tension are discussed. An analytical study based upon solid mechanics is presented in Chapter III together with preliminary results. A description of the experiments performed is presented in Chapter IV together with results from the experiments. The finite element analyses which was performed and the results of those analyses are discussed in Chapter V.

CHAPTER II

LITERATURE SURVEY

Background History

The first study on the effect of nip roller diameter upon a layered structure, a stack of paper, was done by Pfeiffer [4]. In his study he observed that the nip roller produces a strain inducing mechanism which increases the web tension on the outgoing side of the nip roller. He correlated the nip induced tension with the nip load, the diameter of the drum on which the web sheet was wound and the web properties. Pfeiffer noted that as the rolling progresses, the tension in the layered sheets builds to an asymptotic level. Also, a small nip roller was able to produce greater tension. He also suggested that the nip induced tension varies as the inverse square root of the nip roll diameter.

The nip load behavior in his experiments was non-linear with respect to the diameter of the nip roller and the tension induced. An increase in the number of sheets in the stack led to an increase in the nip induced strain. He was able to come to the conclusion that the nip induced stress seeks a constant level during the winding of an actual roll as long as nip force is held constant. Pfeiffer noted in his tests that the sheets nearest to the nip would displace in the direction of the moving nip while some of the sheets near the bottom of the stack would travel in the opposite direction. Using photomicrographs taken from the side of the nip/stack interface, he determined that the instant center of rotation did not lie at the nip/stack interface and in fact it was located beneath the interface in the stack. Sheets above the instant center would travel in the direction of the rolling nip, while the sheets below would travel in the opposite direction.

Recently Good et al [2] have determined the mechanism of nip induced tension. The mechanism is an elongating machine direction strain which exists beneath the nip

roll location on the lower side of the web which is in intimate contact with the wound roll. This elongating strain is due to the compressive Hertzian-like contact stresses which exist through the depth of the web beneath the roller. As the elongating strain advances with the moving nip roll, web material attempts to advance in front of the nip and contract towards the nip in the back of the rolling nip. If the web material in the back of the nip is constrained, a net increase in tension will result due to the nip. It is also mentioned that the nip induced tension cannot exceed the product of kinetic coefficient of friction between the outer wrap & the wrap beneath it, and the nip loading.

Experimental Studies

The experimental observation of the nip induced tension mechanism was originally performed by Pfeiffer and was previously discussed. Good et al [2] performed the first verification of this mechanism with a setup in which a nip roll was driven over a thin strip of aluminum restrained at one end, and strains close to the restrained end were monitored using strain gages. The elongating strain data correlated to the distance moved by the nip roller. It was shown that the nip induced tension tends to saturate after a certain rolling distance. On observing the same phenomenon for different nip roll diameters of 2" & 4", and different nip loads, Good et al [2] were able to explain the reason for the nip induced tension to saturate. A general form for the nip induced stress, they determined experimentally, is of the form :

$$\sigma_x = C_1[1 - e^{-C_2 x}] + C_3 \qquad \{1\}$$

where σ_x represents the total machine direction stress, C_1 represents the saturated value of the nip induced tension, C_2 is the growth rate of the nip induced stress, x is the distance moved by the nip roller, and C_3 is the pre-tension.

They observed the saturation of nip induced stress is due to the fact that nip induced tension exceeded the product of the kinetic friction and nip loading for small nip diameters.

A second experimental verification of this mechanism was performed by Nandakumar [7] on a PSM-4 (Polyurethane rubber) specimen. The method of photo-elasticity was used to observe the behavior of the material when the nip roller moves over it. The experiments were performed with the nip rollers having diameters of 0.5, 0.8 and 1.1 inch. Plots of nip induced stress versus rolling distance were developed for various combinations of nip diameters and nip loads. Two distinct regions of behaviour were noted. The first was a pre-saturation region where the stress kept on increasing as a function of rolling distance and secondly a saturation region where the growth of the nip induced stress is low. There was also an intersection between these two regions where the nip induced stress just began to saturate. He noted that the maximum value of nip induced tension was equal to the product of the dynamic sliding coefficient of friction at the nip contact interface and the nip load. An increase in the nip load for the same diameter nip roller led to an increase in the principal stress along the machine direction. For a uniform increase in nip load, there was a uniform increase in the principal stress in the machine direction.

Nandakumar [7] observed that the saturation value of nip induced tension was reached within a short rolling distance and this is very pronounced as the diameter of the nip roller was made smaller. He also noted that a smaller nip roller can induce more nip induced tension than a large nip roll and subsequently a smaller nip will reach saturation faster if other rolling parameters remain unchanged.

Finite Element Analysis

Pioneering work in the modeling of this complex problem was done by Good et al [2] to analyze and verify their experimental results. Similar models were also performed by Nandakumar [7] and Wu [8] in their studies on nip mechanics. Finite element analysis has proved to be a powerful tool for such analysis. In all these, COSMOS / M™[1] was used to model and carry out the analysis.

The assumptions made while modeling the problem using finite elements were:

1. The problem is considered as a two dimensional plane strain problem as the width of the web is quite large and there is no displacement along the width of the web.
2. The problem is solved in the elastic region.
3. Viscoelasticity is not considered for the web material.
4. There is friction in the interface between the web and the aluminum base plate.

The problem of a nip rolling over an elastic material was approximated as a Hertzian contact problem. A Hertzian parabolic pressure distribution was moved across the surface of the web through time. The lower boundary of the specimen was fully restrained vertically, but only partially restricted horizontally, to accommodate slipping and hence friction.

The web was modeled as two dimensional plane strain elements. Gap elements were introduced at the lower surface to accommodate slippage, which must occur for a nip induced stress to result. Spring elements were introduced at the clamped end to represent the axial stiffness of the web between the nip and the clamped support. In successive time steps, the Hertzian pressure profile was moved to the right one element width.

---

[1] COSMOS / M™, Structural Research and Analysis Corporation, Lincoln Boulevard, Suite 100, Santa Monica, CA 90404.

The most interesting feature observed was that an elongating machine direction (X direction) strain on the lower surface of the web strip exists. The elongating strain on the bottom surface of the web beneath the nip location at each time step was plotted. It was also observed that the strain plot was nearly identical for all the time steps, except that the plot was moved one element to the right at each time step. It was noted that the elongating strain which exists across the nip is due to the combination of the Hertzian pressure profile moving to the right over the upper surface and the frictional forces on the lower surface. Hence, the area under the strain plot is a measure of the deformation contribution from the nip rolling over a specific element. This was converted to the deformation contribution due to unit displacement of the nip roller. Good et al[2] formulated an equation for the strain in the web as:

$$\varepsilon_x = \frac{C * x}{L_i + x} \qquad \{2\}$$

Where C is the deformation contribution due to unit displacement of the nip roller, x is the total nip rolling distance and L_i is the initial distance between the clamped support and the nip roller prier to rolling.

For large rolling displacements, the nip induced strain predicted from equation {2} will approach a constant value. From earlier observations, it is seen that this constant value is dependent on the coefficient of friction and the nip load. Therefore, equation {2} can be used for predicting the nip induced strain for the cases in which the saturated value of nip induced tension has not been achieved.

Summary

Earlier studies in nip mechanics' mechanism have indicated that the nip induced tension is dependent on the nip diameter. The rate of nip induced tension is the derivative of the nip induced tension with respect to the rolling distance. It was observed that more tension was produced when small diameter nips were used. The nip induced tension has been shown to reach the saturated value within one revolution of the winding roll with small diameter nips, and the saturation is due to the fact that the nip induced tension has reached the limit of the product of kinetic coefficient of friction and the nip load. Large nip diameters may prevent the nip induced tension from reaching its saturated value within one revolution of the wound roll, and the value of nip induced tension may not reach the limit of the product of kinetic coefficient of friction and the nip load even after rolling large distances. Hence, an attempt will be made to study the effect of large nip rollers on the nip induced tension and hence the rate of nip induced tension.

CHAPTER III

ANALYTICAL STUDY

Objective

The objective of this study is to determine the effect of nip diameter on the rate of nip induced tension. This is achieved by considering different combinations of nip diameters and nip loads.

Approach to the problem

The nip roller along with nip load can be modeled as a Hertzian contact problem. When two cylindrical bodies are in contact (fig. 2), the contacting area is a rectangle whose half width is a function of the force pressing the cylinders together, the moduli of elasticity of the cylinders, the poisson's ratio, the width of contacting cylinders and the diameters. This is given by the equation (Shigley [6]) :

$$b = \sqrt{\frac{2P}{\pi l} \frac{[(1 - \upsilon_1^2) / E_1] + [1 - \upsilon_2^2) / E_2]}{(1 / d_1) + (1 / d_2)}} \qquad \{3\}$$

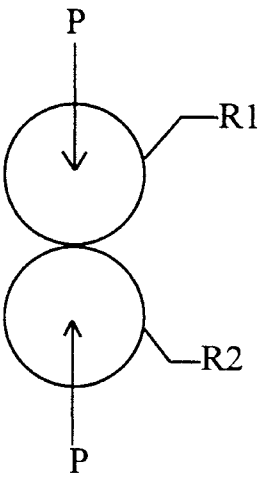

Two Cylinders in contact

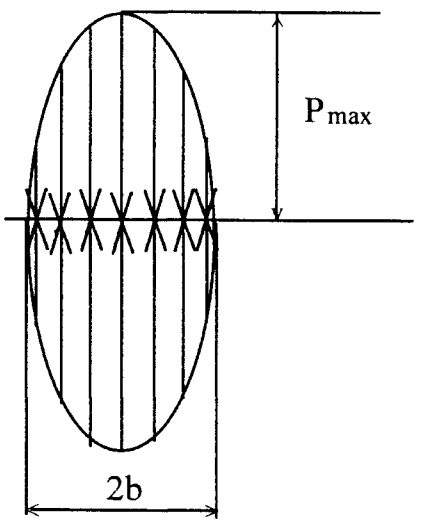

Hertzian contact pressure profile

Fig. 2 Contact of two cylindrical surfaces

In this study, the diameter of the first cylinder is the diameter of the nip roller, and the second cylinder is the infinite half plane represented by the web (fig. 3)

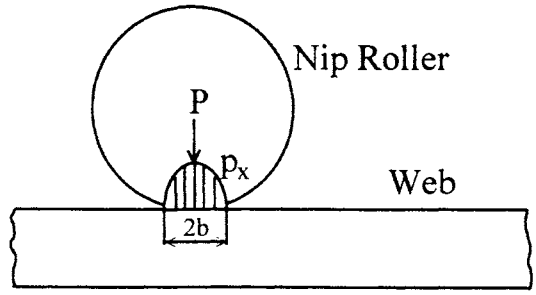

Fig. 3 Pressure Profile on Contact Surface

The web acted upon by a nip roller can be modeled as a specimen acted upon by a Hertzian pressure distribution, which is assumed to be elliptical and is given by the equation (Radzimovsky [5]):

$$p_x = \frac{2P}{\pi b^2 l}\sqrt{b^2 - x^2} \qquad \{4\}$$

The maximum Hertzian contact pressure is given by :

$$p_{max} = \frac{2P}{\pi b l} \qquad \{5\}$$

The stress in the web is due to the superposition of : (i) The Hertzian distribution of pressure on the surface and (ii) The biaxial tension due to the applied load (Johnson [3]). Hence the longitudinal strain in the web is given by:

$$\varepsilon_x = \frac{1 - \upsilon^2}{E}\{\sigma_x + \frac{\upsilon}{1 - \upsilon^2} p_x\} \qquad \{6\}$$

The Hertzian semi contact width and the Hertzian pressure profile were calculated for web material, newsprint paper of 9.69 inch wide and 0.0017 inch thick. The calculations were made for different nip diameters ranging from 4 inch to 60 inch, with the nip loads of 2.27 pli, 2.8 pli, 8.26 pli, 11.4 pli and 24 pli.

Results of Analysis

The estimated nip induced stress for 1 inch rolling of nip roller is shown for various nip diameters in figs. 4, 5, 6 & 7 respectively for 2.8 pli, 8.26 pli, 11.4 pli and 24 pli nip load. Since, the stress in the web after rolling is nominally uniform, the uniaxial form of Hooke's Law ($\sigma_x = E\varepsilon_x$) was applied to convert machine direction strains to stresses. A comparison of nip induced stress is made in fig. 8 for various nip loads. It may be seen that smaller diameter nips induce higher stress in the web compared to the larger diameter nips, for the same rolling distance and nip load. This is similar to the observations made by Good et al[2] and Nandakumar[7].

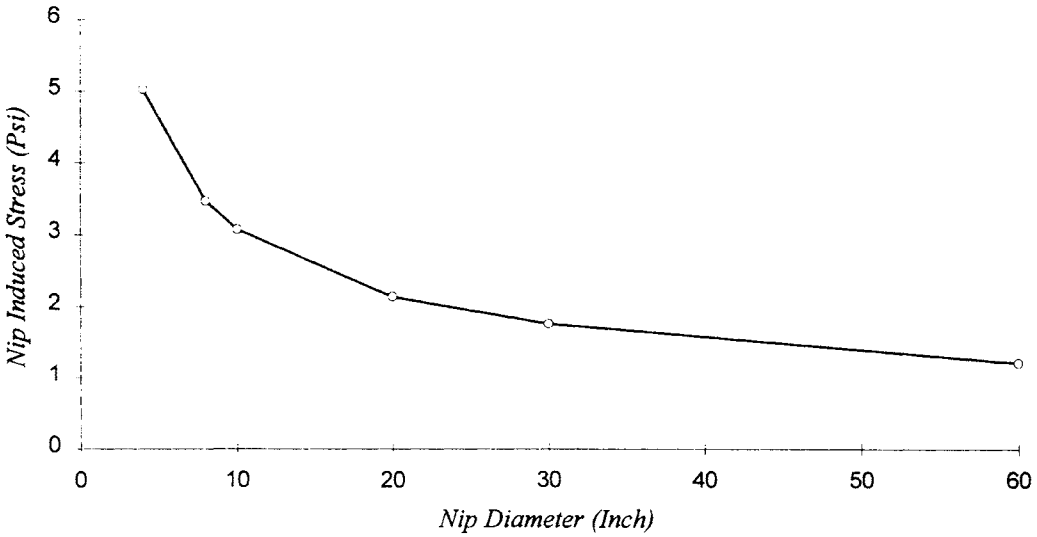

Fig. 4 Estimated Nip Induced Stress

for 1 inch Rolling, with 2.8 pli Nip Load

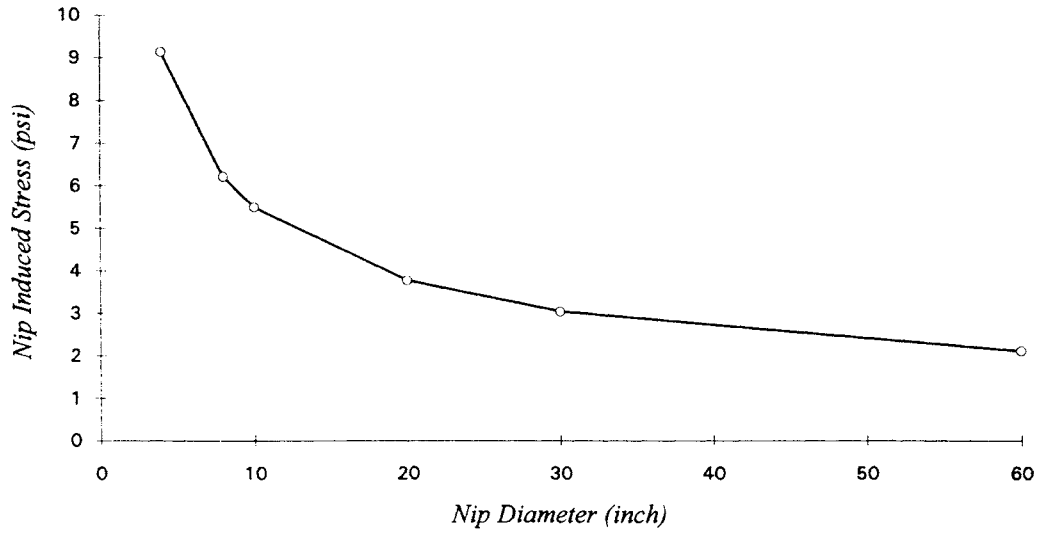

Fig. 5 Estimated Nip Induced Stress

for 1 inch Rolling, with 8.26 pli Nip Load

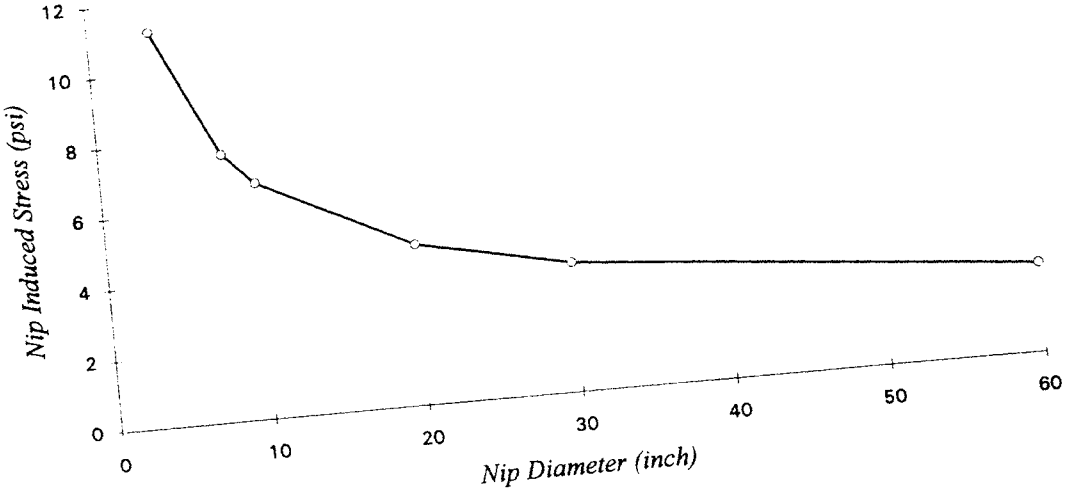

Fig. 6 Estimated Nip Induced Stress for 1 inch Rolling, with 11.77 pli Nip Load

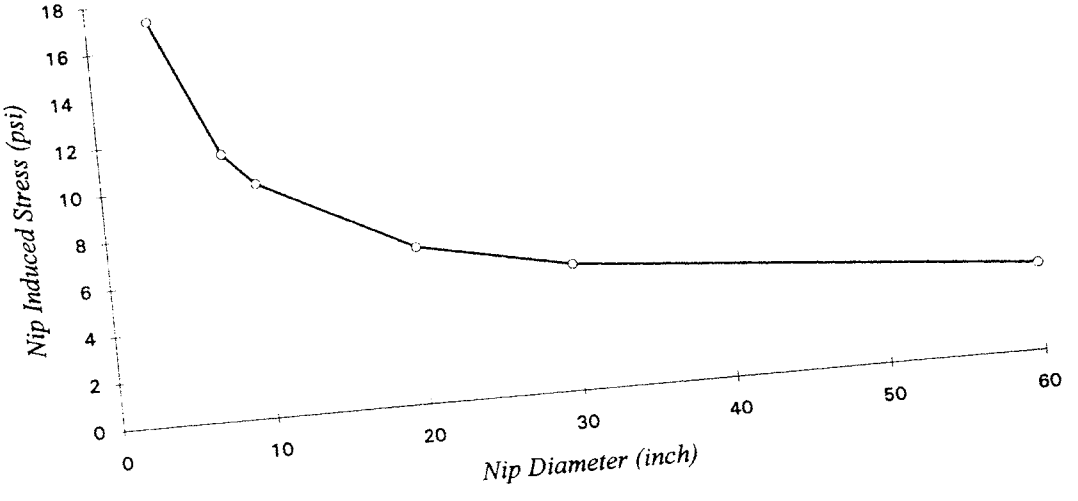

Fig. 7 Estimated Nip Induced Stress for 1 inch Rolling, with 24 pli Nip Load

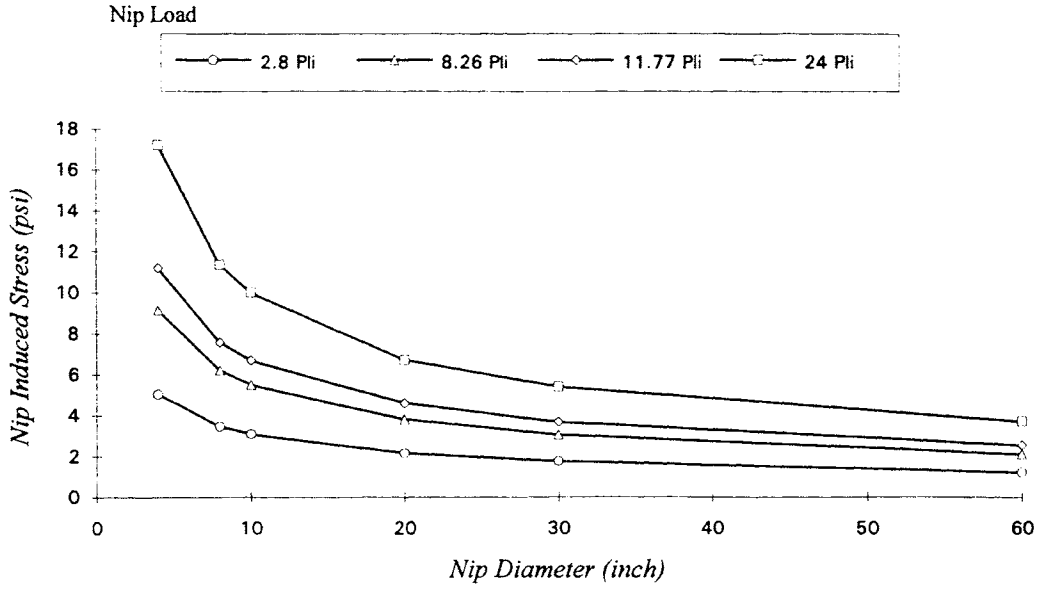

Fig. 8 Comparison of Nip Induced Stress for 1 inch Rolling, with different Nip Diameters

The nip induced stress for distance rolled with various diameter nips is shown in figs. 9, 10, 11 & 12 respectively for 2.8 pli, 8.26 pli, 11.4 pli and 24 pli nip load. It may be noted that the nip induced stress rises rapidly for smaller diameter nips when compared to larger ones.

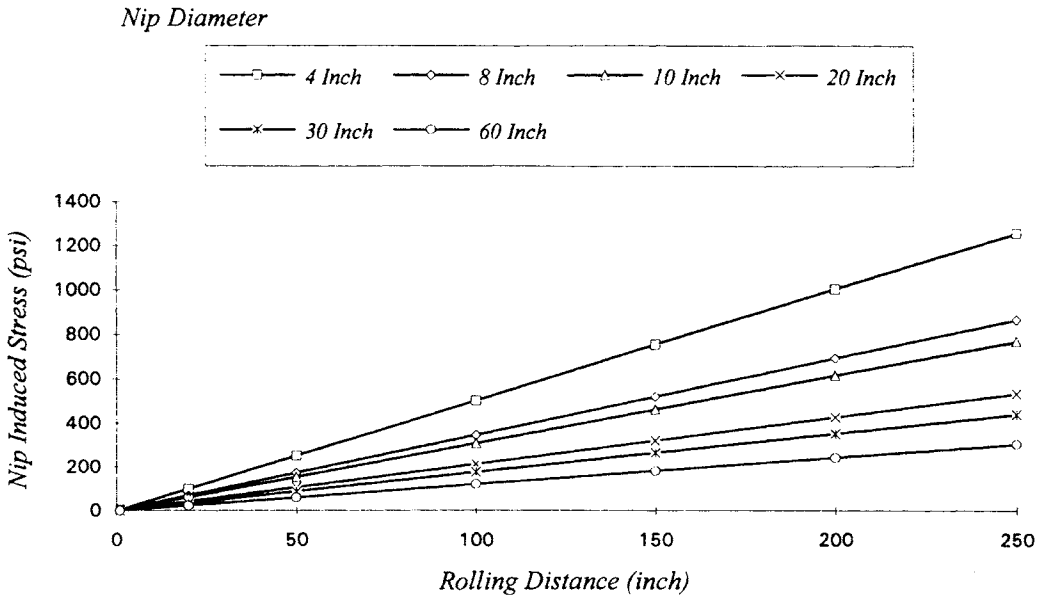

Fig. 9 Comparison of Estimated Nip Induced Stress for 2.8 pli Nip Load

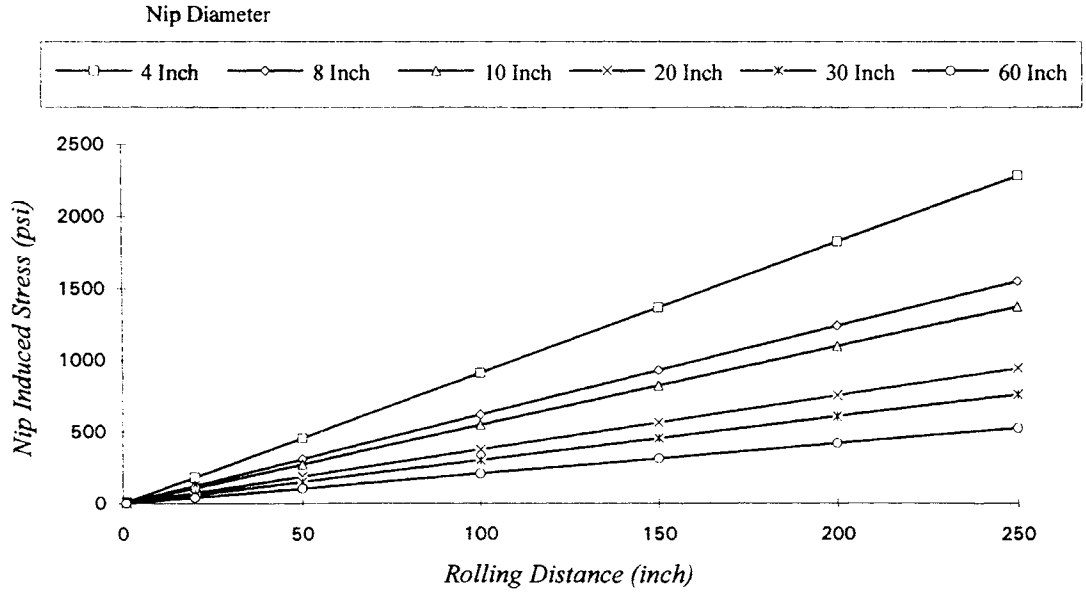

Fig. 10 Comparison of Nip Induced Stress for 8.26 pli Nip Load

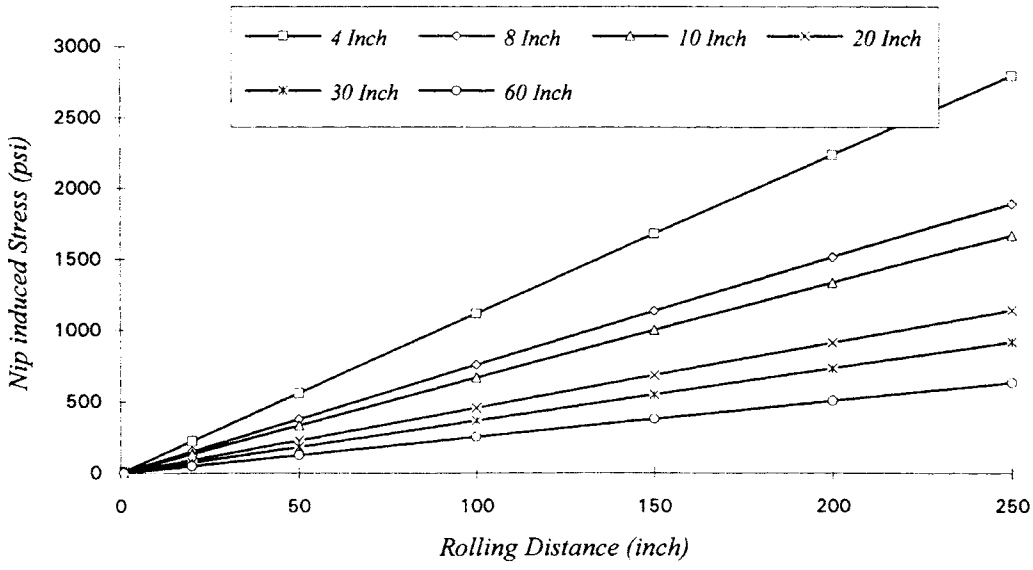

Fig. 11 Comparison of Nip Induced Stress for 11.77 pli Nip load

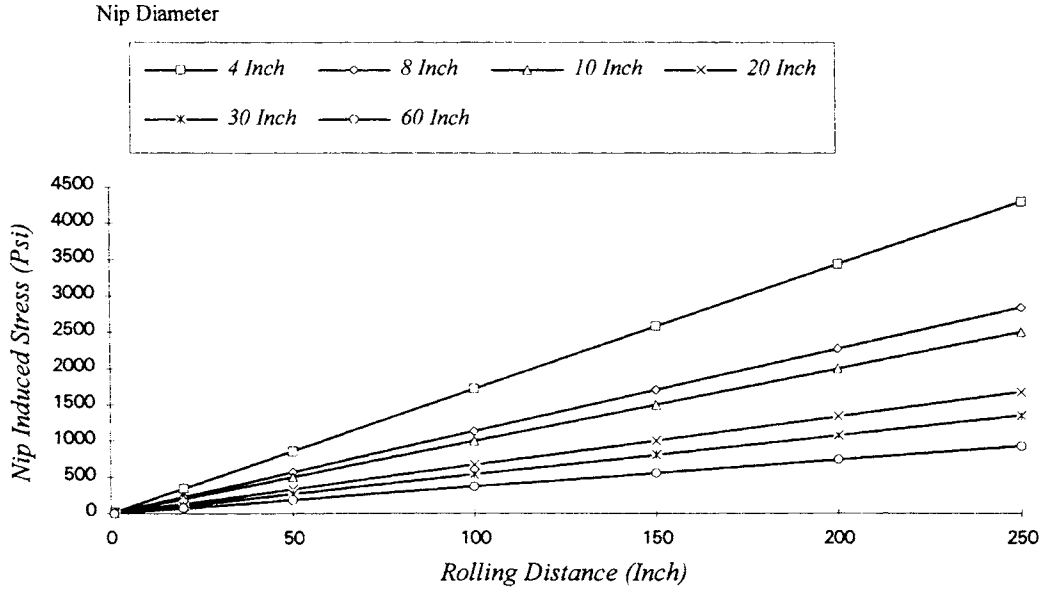

Fig. 12 Comparison of Nip Induced Stress for 24 pli Nip Load

Hence, for a given nip load, the nip induced tension with a small diameter nip rises until it reaches the limit of the product of coefficient of friction and the nip load. If the nip diameter is large, the rise in the nip induced stress is very slow, and it may not reach the saturated value even after large rolling distances.

CHAPTER IV

EXPERIMENTAL ANALYSIS

Experimental study

The experimental study to determine the effect of nip diameter on the rate of nip induced tension was carried out on a newsprint paper web (E= 800 ksi, υ = 0.01), 9.865 inch wide and 0.0017 inch thick. In the earlier experiments by Good et al [2] on aluminum strip and Nandakumar [7] on PSM-4 specimen, small diameter nips were employed and, also, the length of nip traversal was small due to the experimental set-up limitations. In order to accommodate large diameter nips and also to increase the nip traversal distance, the new experimental set-up was developed [fig. 13].

The important features of this set-up are :

1. nip roller can traverse 95 inches in a single pass.
2. nip rollers up to 60 inch diameter can be accommodated to carry out experiments.
3. The set-up can accommodate multiple layers of web and the nip induced stress in each of the eight layers can be recorded simultaneously.

Since the deformations are small, a precise means of measuring the nip induced tension had to be incorporated. The web was placed on the flat bed and one end of the web was connected to the strain gage and the other end was held under a pre-tension by means of dead weights, just to keep the web aligned on the flat bed. The pre-tension can be varied to simulate the effects of incoming web tension on nip induced tension. A dead weight of 1 lbf was used in all experiments which provided a pre-tension of 61 psi in the web prior to rolling.

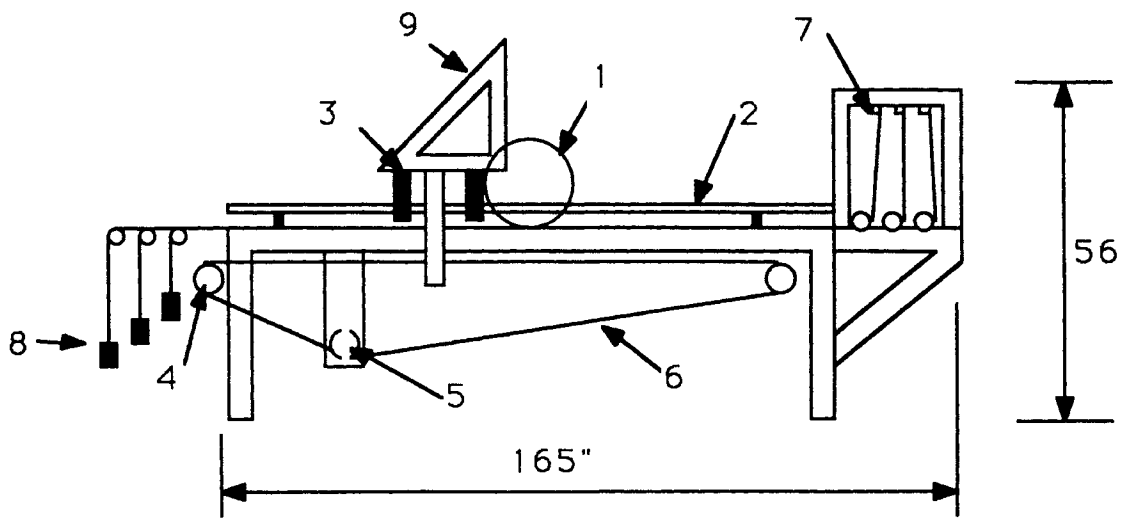

1. Nip Roller
2. Guide Rail
3. Linear Bearing
4. Drive Motor
5. Displacement Transducer
6. Driving Belt
7. Strain Gage
8. Dead Weights for Pre- tension
9. Carriage for fixing Nip Roller

Fig. 13 Experimental Set-up

The nip roller was rolled over the web starting from the strain gage end. The strain gages on the load cells were connected in a Wheatstone bridge network to cancel any strains due to bending that might occur. A displacement transducer was used to measure the nip roller displacement from the starting position.

The strain gage bridge and the displacement transducer were connected to the Keithley data acquisition system, which is connected to an IBM PC. This scheme allows the simultaneous recording of the nip roller position and the nip induced tension.

Experiments were conducted using nip rollers of 8 inch (with 2.27, 2.8 & 8.26 pli nip load), 10 inch (with 2.8 & 8.26 pli nip load), 20 inch (with 8.26, 11.77 & 24 pli nip load), 30 inch (11.77 & 24 pli nip load) and 60 inch (with 24 pli nip load). The combination of nip diameter of 20 inch and the nip load of 24 pli exerted a maximum contact stress of 756 psi. Since the yield strength of the paper is of the order of 2500 psi (at 5% offset), the stresses exerted upon the paper web during all the experiments were definitely within the elastic range.

Since the nip roller diameters were large, the saturated value of nip induced stress was not reached even after the nip traversal of 95 inches. Hence, to observe the trend, multiple passes were made by clamping the edge of the web after each pass, raising the nip roller and returning to the start position, lowering the nip roller and releasing the clamps, and then resuming the experiment.

Results of Experiments

The results of the experiment are plotted and are shown in Fig. 14 through 24. A comparison of these results is made in fig. 25, 26, 27 & 28 respectively for 2.8 pli, 8.26 pli, 11.77 pli and 24 pli. These plots indicate that for a given nip load, smaller diameter nips produce more stress compared to large diameter nips. In the pre-saturation region,

the slope of the curve is larger for a smaller diameter nip roller than for a large diameter nip roller, with the same nip load. This result is similar to what was observed by Good et al [2], Nandakumar [7] and Wu [8].

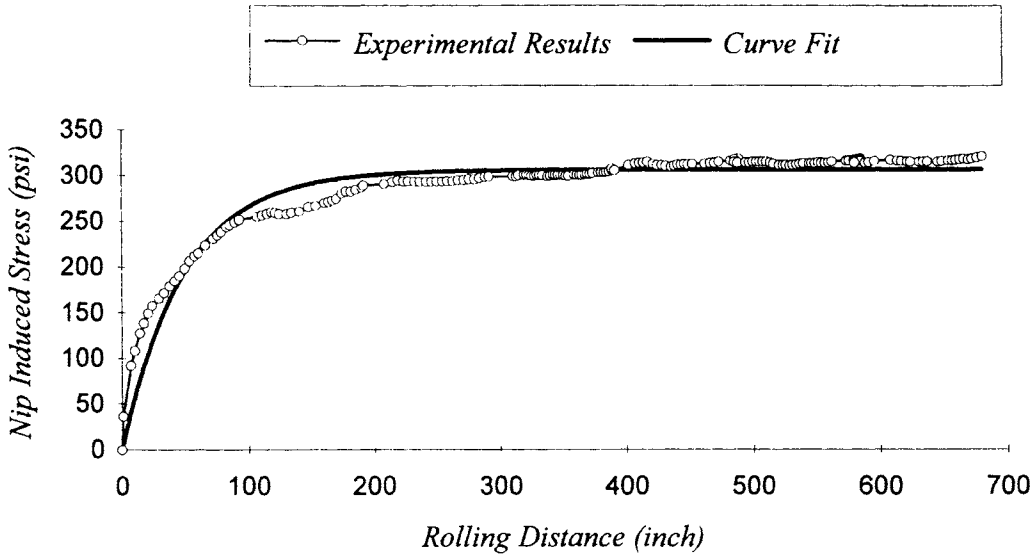

$$\sigma_x = C_1[1 - e^{-C_2 x}]$$

From Curve Fit, $C_1 = 305.86$ & $C_2 = 0.02$

Fig. 14 nip Induced Stress Vs Rolling Distance for 8 inch Diameter nip and 2.27 pli nip Load

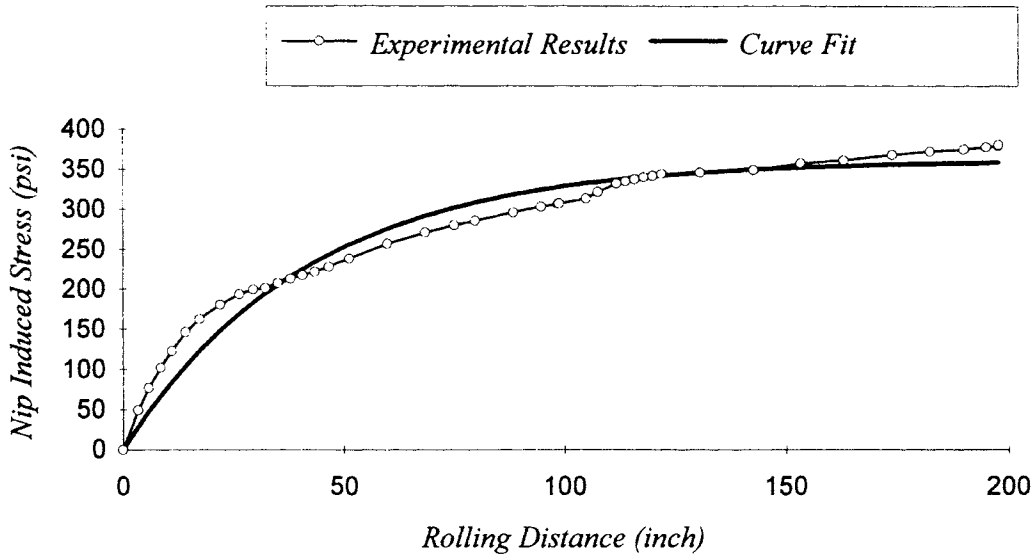

$$\sigma_x = C_1[1 - e^{-C_2 x}]$$

From Curve Fit, $C_1 = 362.17$

$C_2 = 0.024$

Fig. 15 nip Induced Stress Vs Rolling Distance for 8 inch Diameter nip and 2.8 pli nip Load

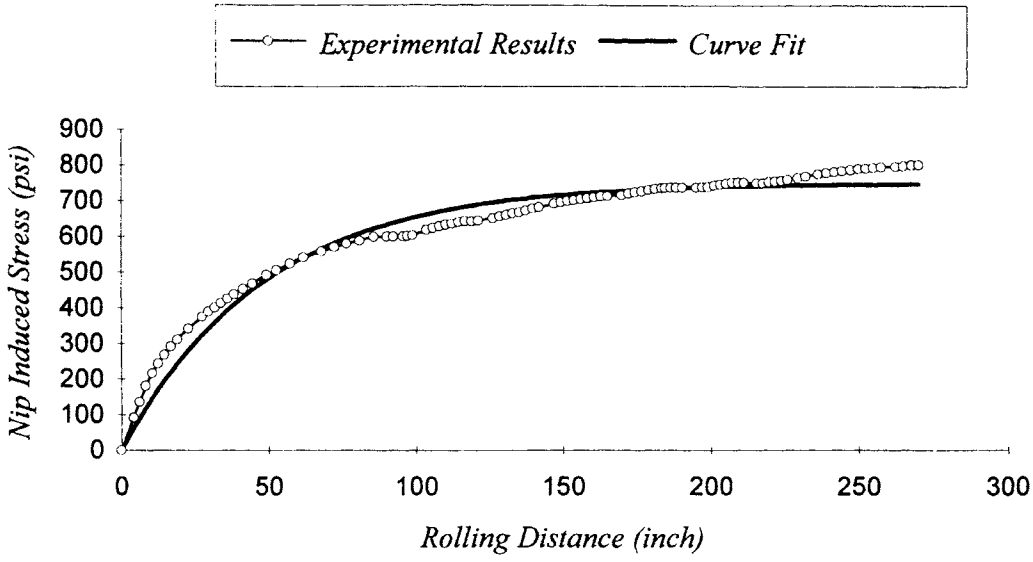

$$\sigma_x = C_1[1 - e^{-C_2 x}]$$

From Curve Fit, $C_1 = 750.86$

$C_2 = 0.02$

Fig. 16 nip Induced Stress Vs Rolling Distance for 8 inch Diameter nip and 8.26 pli nip Load

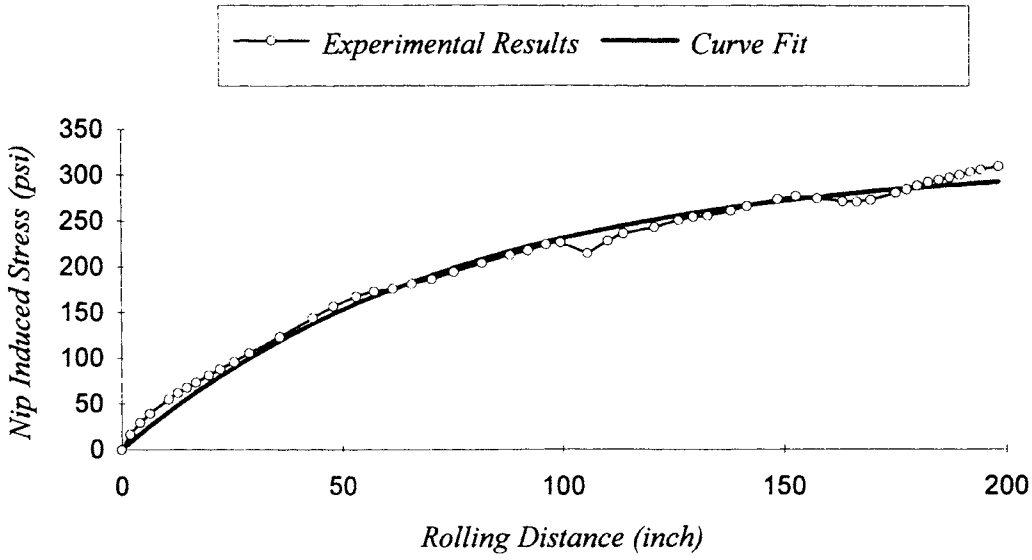

$$\sigma_x = C_1[1 - e^{-C_2 x}]$$

From Curve Fit, $C_1 = 315.48$

$C_2 = 0.013$

Fig. 17 nip Induced Stress Vs Rolling Distance for 10 inch Diameter nip and 2.8 pli nip Load

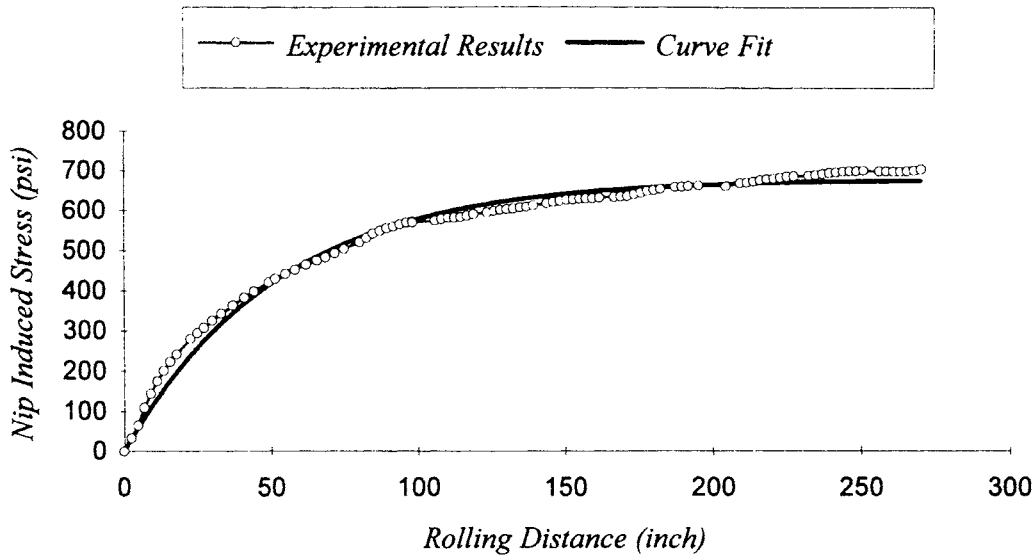

$$\sigma_x = C_1[1 - e^{-C_2 x}]$$

From Curve Fit, $C_1 = 679.17$

$C_2 = 0.019$

Fig. 18 nip Induced Stress Vs Rolling Distance for 10 inch Diameter nip and 8.26 pli nip Load

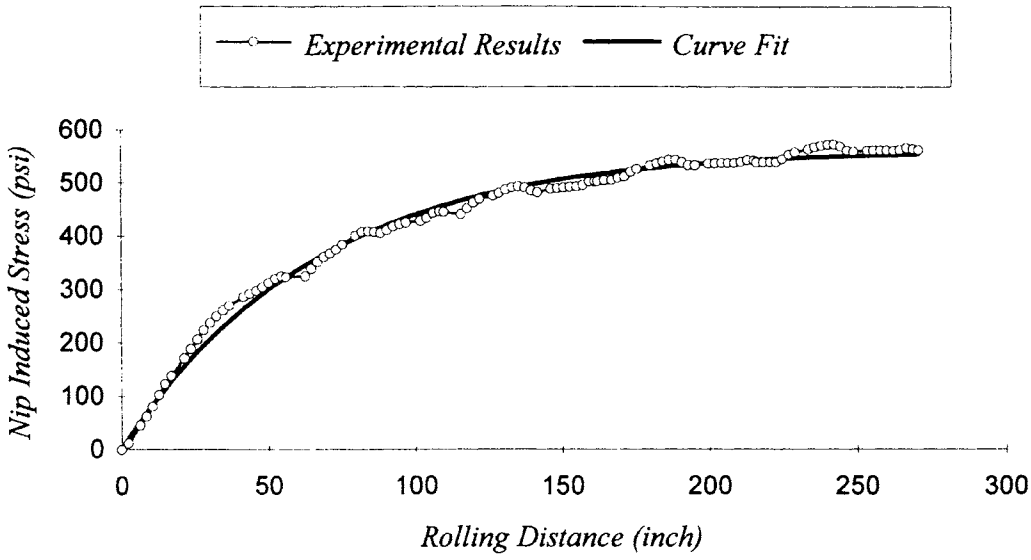

$$\sigma_x = C_1[1 - e^{-C_2 x}]$$

From Curve Fit, $C_1 = 563.27$

$C_2 = 0.015$

Fig. 19 nip Induced Stress Vs Rolling Distance for 20 inch Diameter nip and 8.26 pli nip Load

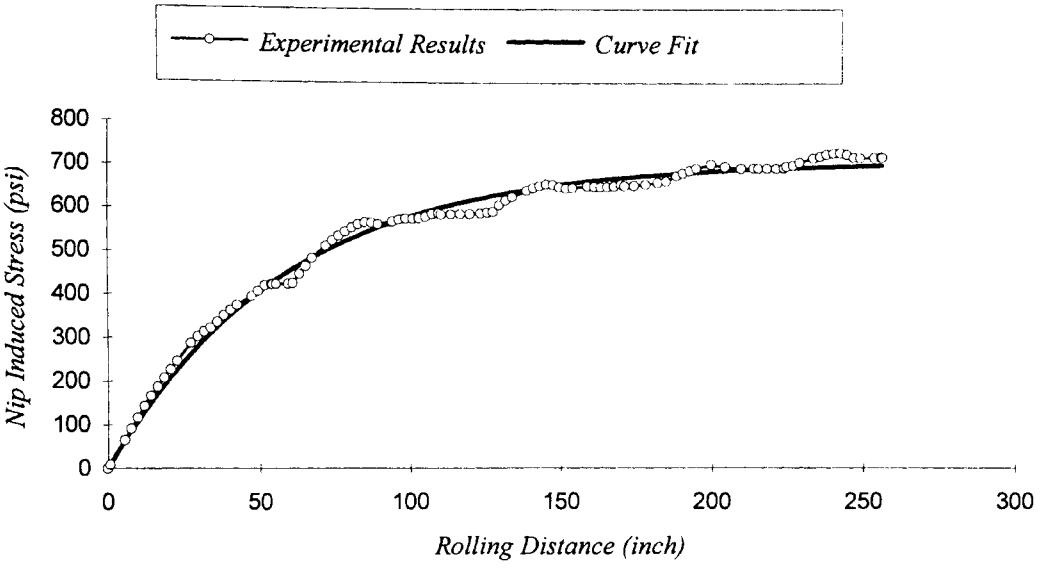

$$\sigma_x = C_1[1 - e^{-C_2 x}]$$

From Curve Fit, $C_1 = 710.28$

$C_2 = 0.017$

Fig. 20 nip Induced Stress Vs Rolling Distance for 20 inch Diameter nip and 11.77 pli nip Load

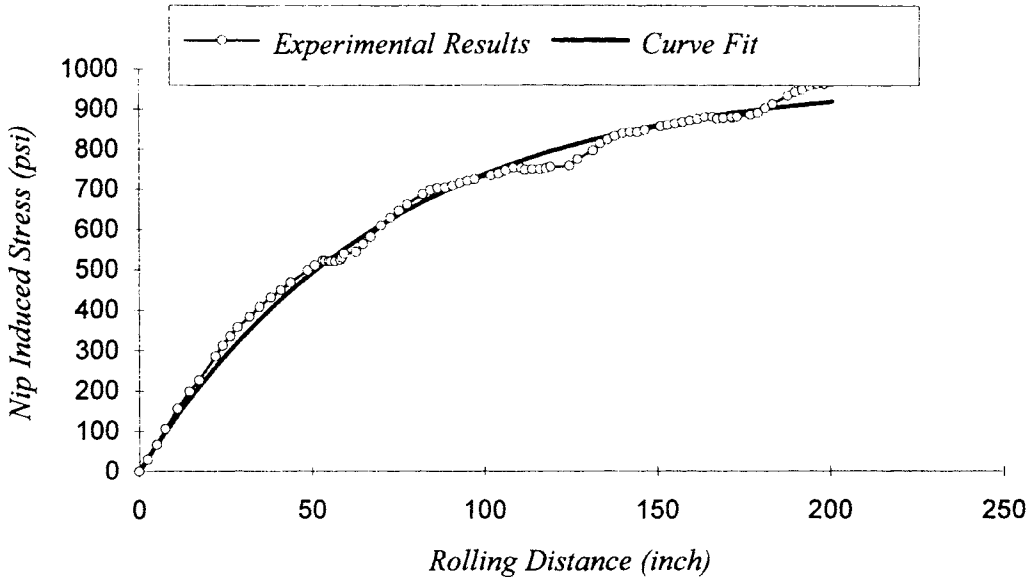

$$\sigma_x = C_1[1 - e^{-C_2 x}]$$

From Curve Fit, $C_1 = 979.24$

$C_2 = 0.014$

Fig. 21 nip Induced Stress Vs Rolling Distance for 20 inch Diameter nip and 24 pli nip Load

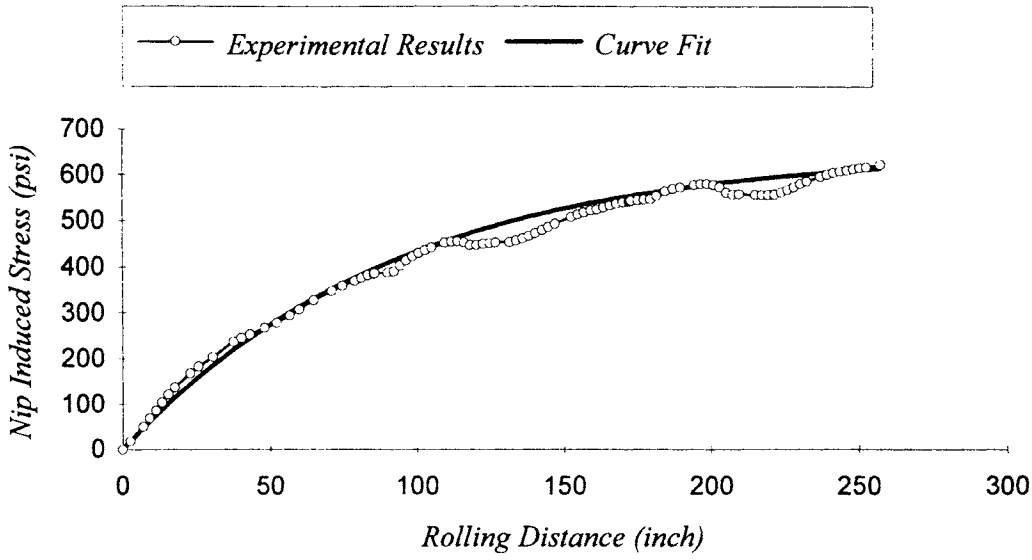

$$\sigma_x = C_1[1 - e^{-C_2 x}]$$

From Curve Fit, $C_1 = 635.27$

$C_2 = 0.01$

Fig. 22 nip Induced Stress Vs Rolling Distance for 30 inch Diameter nip and 11.77 pli nip Load

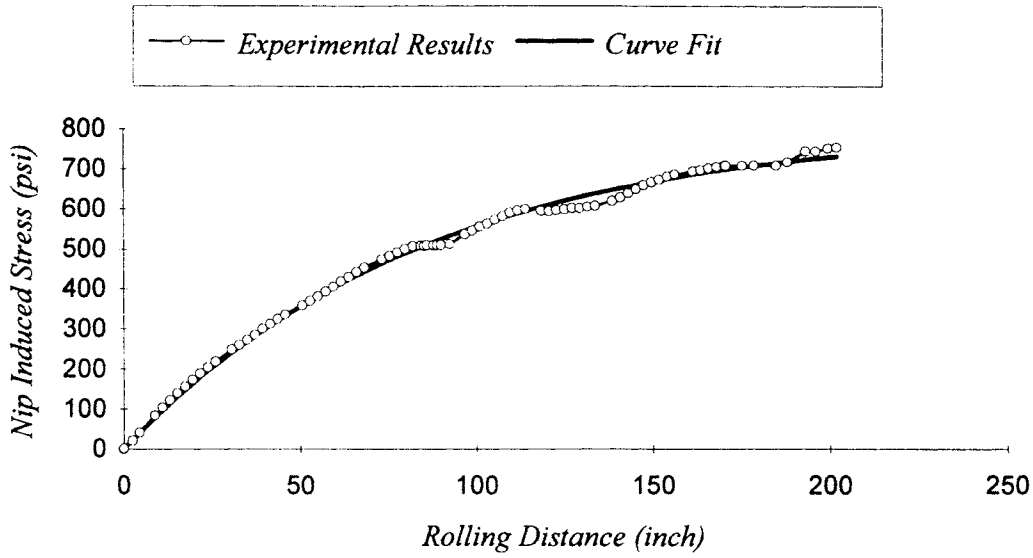

$$\sigma_x = C_1[1 - e^{-C_2 x}]$$

From Curve Fit, $C_1 = 808.24$

$C_2 = 0.011$

Fig. 23 nip Induced Stress Vs Rolling Distance for 30 inch Diameter nip and 24 pli nip Load

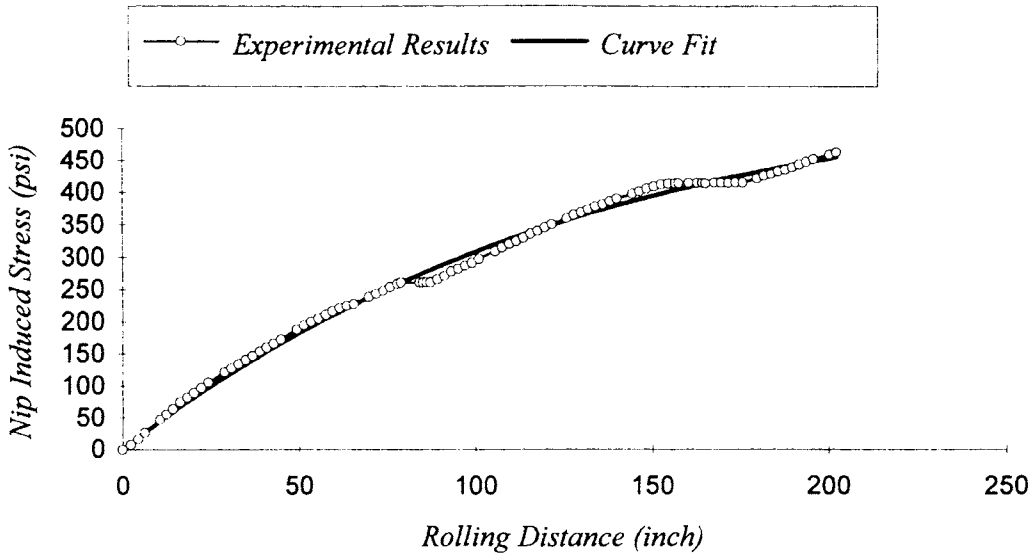

$$\sigma_x = C_1[1 - e^{-C_2 x}]$$

From Curve Fit, $C_1 = 582.48$

$C_2 = 0.007$

Fig. 24 nip Induced Stress Vs Rolling Distance for 60 inch Diameter nip and 24 pli nip Load

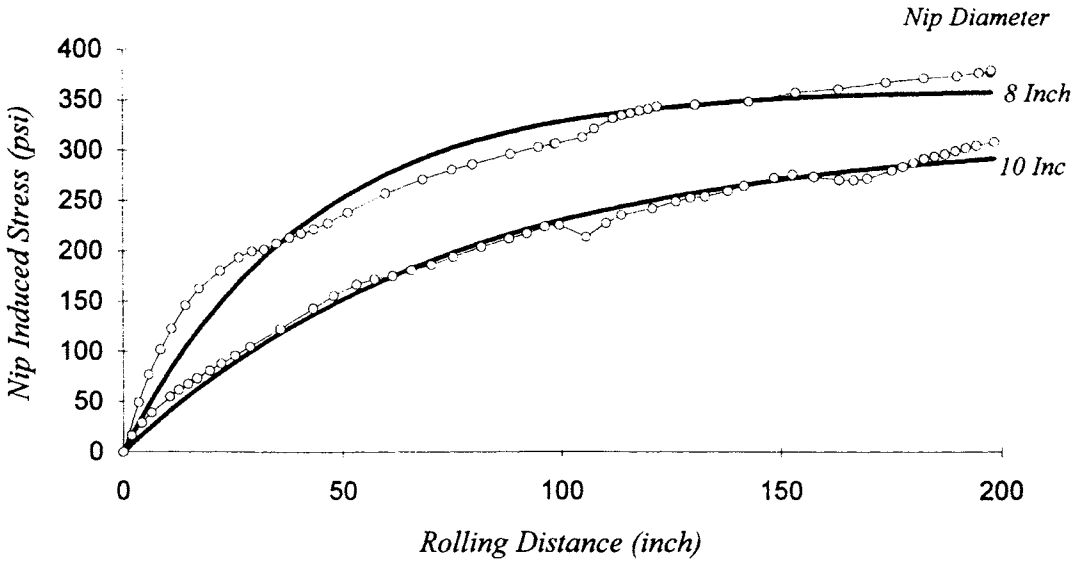

Fig. 25 Comparison of Experimental Results for 2.8 pli nip Load

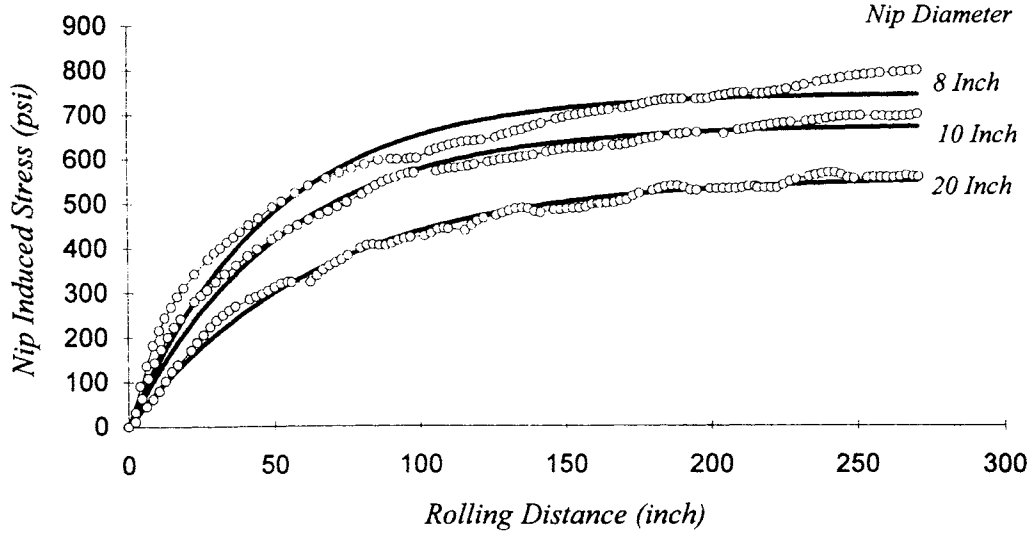

Fig. 26 Comparison of Experimental Results for 8.26 pli nip Load

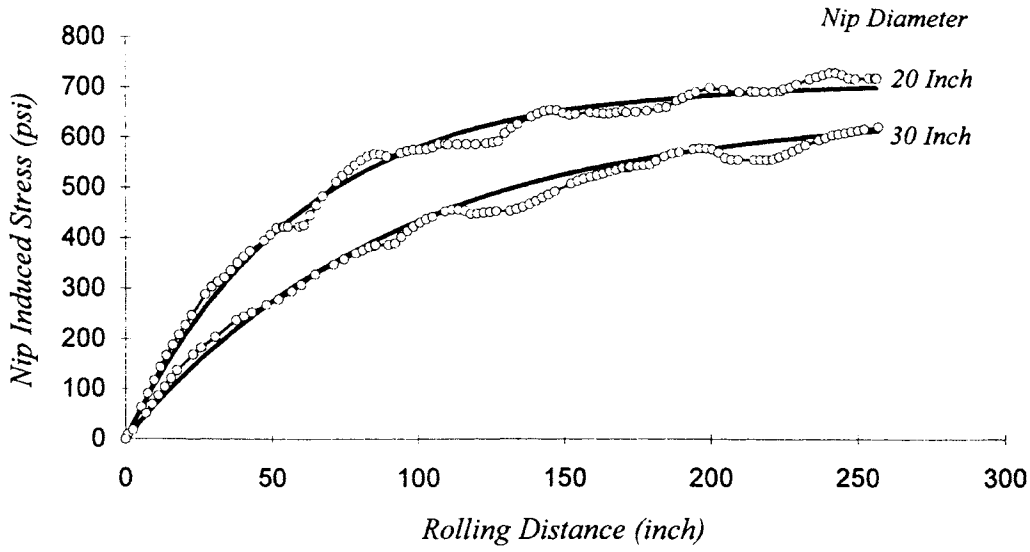

Fig. 27 Comparison of Experimental Results for 11.77 pli nip Load

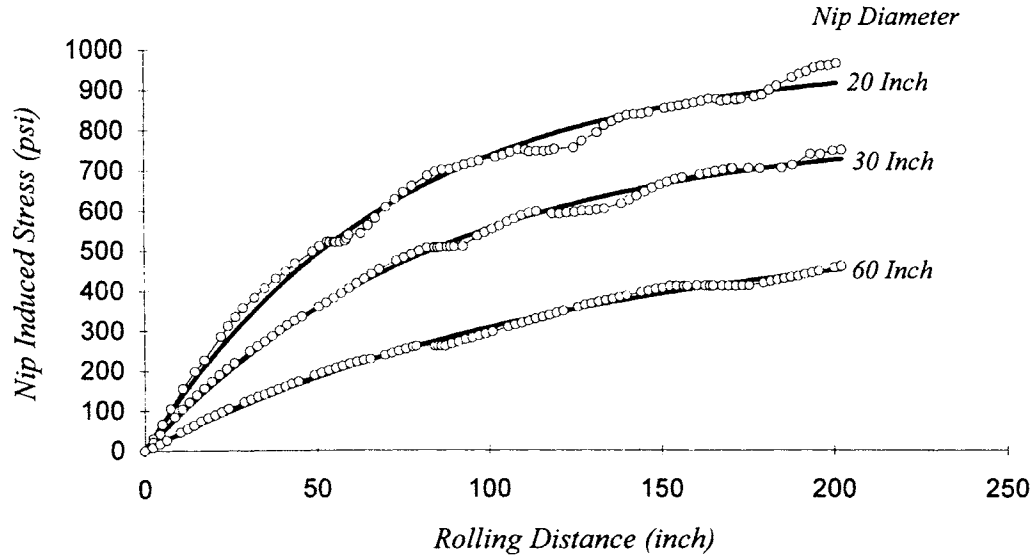

Fig. 28 Comparison of Experimental Results for 24 pli nip Load

A general form of nip induced stress given by Good et al [2] is of the form :

$$\sigma_x = C_1[1 - e^{-C_2 \cdot x}] + C_3 \qquad \{7\}$$

Where σ_x represents the total machine direction stress, C_1 represents the saturated value of the nip induced tension, C_2 is the growth rate of the nip induced stress, x is the distance moved by the nip roller, C_3 is the pre-tension. In this case $C_3 = 61$ as in all the experiments a pre-tension of 61 psi is used.

The values obtained for C_1 & C_2 on fitting the curve for all the experimental results is presented in Tables I & II.

nip Diameter (inch)	nip Load (pli)	C_1	C_2
8	2.27	305.86	0.02
	2.8	362.17	0.02
	8.26	750.86	0.02
10	2.8	315.48	0.013
	8.26	679.17	0.019
20	8.26	563.27	0.015
	11.77	710.28	0.017
	24	979.24	0.014
30	11.77	635.27	0.01
	24	808.24	0.011
60	24	582.48	0.007

Table I. Values of C_1 and C_2 from experimental results based on nip Diameter

nip Load (pli)	nip Diameter (inch)	C_1	C_2
2.27	8	305.86	0.02
2.8	8	362.17	0.02
	10	315.48	0.013
8.26	8	750.86	0.02
	10	679.17	0.019
	20	563.27	0.015
11.77	20	710.28	0.017
	30	635.27	0.01
24	20	979.24	0.014
	30	808.24	0.011
	60	582.48	0.007

Table II. Values of C_1 and C_2 from experimental results based on nip Load

It may be observed from Tables (I) &(II) that the saturated value of nip induced stress(C_1) is dependent on both nip load and nip diameter. Whereas the growth rate parameter (C_2) varies with nip diameter. On comparing the growth rates for various nip diameters, it can be observed that the growth rate for a smaller diameter nip roller is higher and also for a given nip diameter, the growth rate remains more or less a constant and is independent of nip load.

CHAPTER V

FINITE ELEMENT ANALYSIS

Modeling Details

A finite element package, ANSYS™[1] , was used for modeling and analysis. Since the width of the web was quite large compared to the thickness (9.685 inch Vs 0.0017 inch), the web was assumed to conform to plane strain conditions. Hence, the web under the action of a nip was modeled as two dimensional plane strain elements acted upon by a Hertzian pressure profile on the upper surface. Interface elements were used to accommodate slippage between the web and the flat-bed. 2D spar elements were used to simulate the axial stiffness of the web between the nip and the clamped surface.

Fig. 29 shows the detail of the model. 1200 plane strain elements (0.000844 inch wide & 0.00017 inch thick) represent the web. 121 Interface elements were introduced at the lower surface of the web to accommodate the slippage between the web and the flat-bed. Eleven, 2D Spar elements were introduced at the end which represents the axial stiffness of the web between the nip and the clamped support(a distance of 30 inches). In successive steps, the Hertzian pressure profile was moved to the right one element width.

---

[1] ANSYS™, Swanson Analysis Systems Inc., P.O.Box 65, Houston, PA 15342

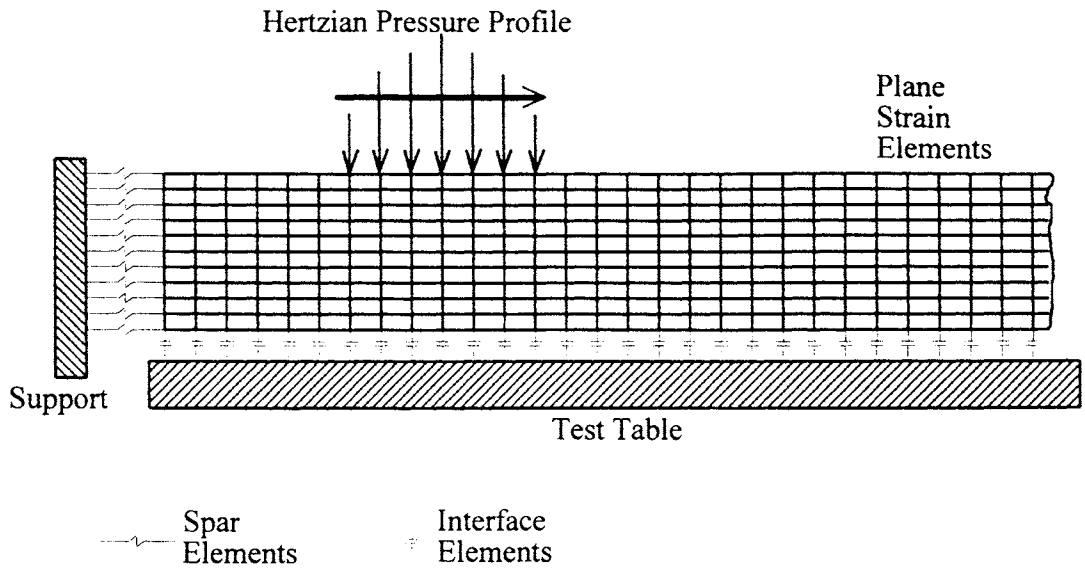

Fig. 29 Finite Element Model

Analysis for 8 inch nip roller and 2.8 pli nip Load

The combination of 8 inch diameter nip and 2.8 pli nip Load resulted in a semi contact width (b) of 0.00435 inches, and the equation for the pressure distribution as per equation {4} is :

$$p_x = 9.379 * 10^4 * (1.8923 * 10^{-5} - x^2)^{1/2} \qquad \{8\}$$

With this, the load acting on each element is evaluated by integrating the pressure distribution equation between the appropriate limits (fig. 30). For example, the load acting on the middle element is given by :

$$F_6 = \int_{-4.225*10^{-4}}^{+4.225*10^{-4}} p_x \, dx = 0.343 Lbf \qquad \{9\}$$

or, in terms of pressure load, 0.343/8.4375E-4 = 407 psi.

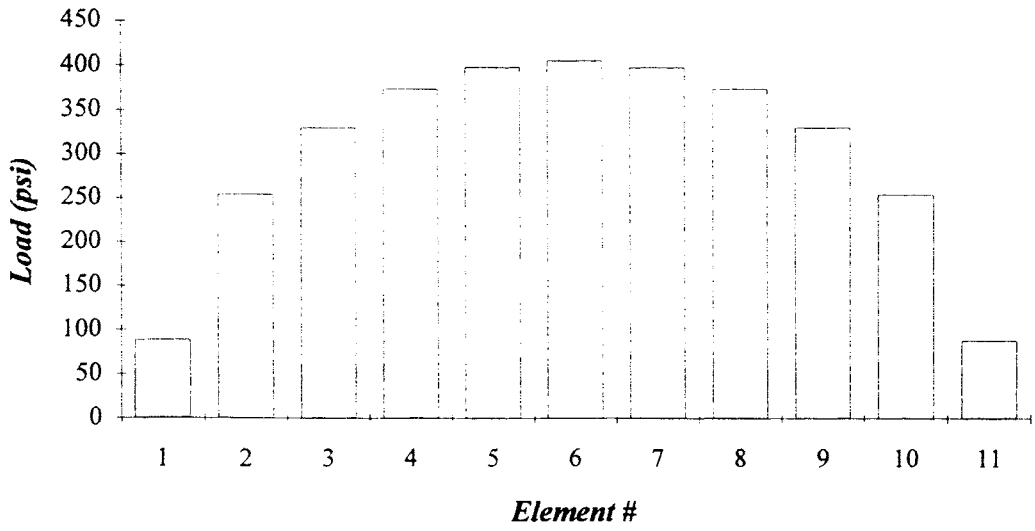

Fig. 30 Load Distribution on the Elements

Likewise, the load acting on each element is evaluated and is input to ANSYS. In the successive time steps, the load profile is moved to the right by one element width (ANSYS code is given in Appendix). The elongating machine direction strain on the lower surface of the web strip beneath the nip location is noted for each time step. The strain plot at the eleventh time step is shown in fig. 31. At the following time step, the plot would be nearly identical except that the curve would have moved by one elemental distance to the right. This shows that an elongating machine direction strain exists in the web due to the combination of the Hertzian pressure profile moving to the right over the upper surface of the web strip and the frictional forces on the lower surface. As the nip passes over the web strip, every point on the lower surface witnesses the elongating strain distribution shown in Fig. 31 and the extension of the web strip due to the nip rolling over one finite element will be the integral of the strain, which is equivalent to the area under the curve in Fig. 31. The area under the curve is found to be $2.5388*10^{-7}$ inch, which is the deformation contribution from the nip rolling over an element which is 0.000844 inch in width. The deformation due to the nip roll moving 1 inch will be $2.5388*10^{-7} inch$ *

$(1\ inch / 0.000844\ inch)$ or $3.0*10^{-4} inch$ for every 1 inch of rolling distance. The strain in the web strip can be calculated from equation {2} formulated by Good et al [2].

$$\varepsilon_x = \frac{c*x}{L_i + x} = \frac{3.0*10^{-4}*x}{L_i + x} \qquad \{10\}$$

Where L_i is the initial distance between the clamped support and the nip roll prior to rolling(inch). Note that equation {10} is nonlinear with respect to the nip rolling displacement and is of the similar form as equation {7}.

The finite element analysis is performed for nip diameters of 8 inch (with 2.8 & 8.26 pli nip load), 10 inch (with 2.8 & 8.26 pli nip load), 20 inch (with 8.26, 11.77 & 24 pli nip load), 30 inch (with 11.77 & 24 pli nip load) and 60 inch (with 24 pli nip load) to observe the effect of nip diameter on the nip induced strain. For each of the analysis, elongating machine direction strain on the lower surface of the web beneath the nip location is noted and is plotted.

Results of Analysis

The strain plots resulted from the finite element analysis performed are presented in fig. 31 through fig. 43. These plots are the strains observed in the bottom layer of the web.

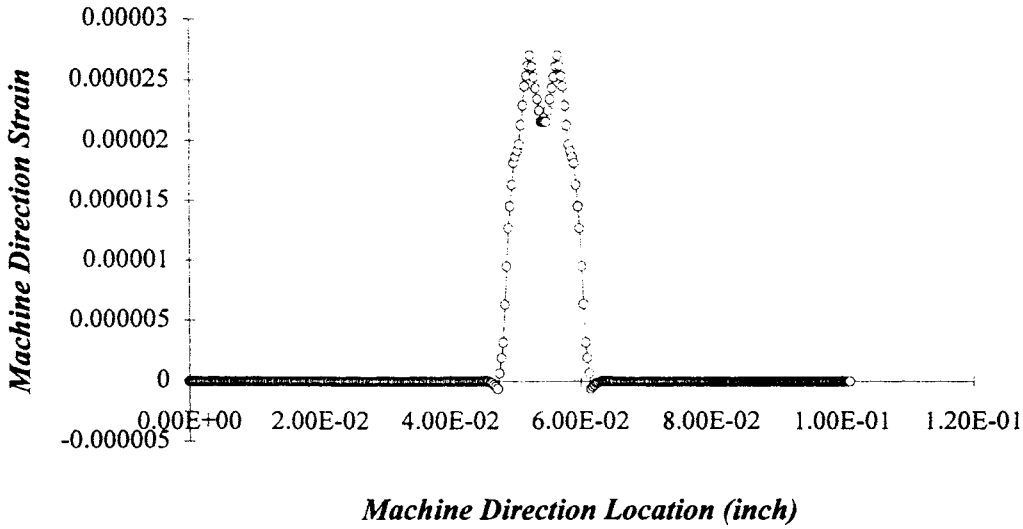

Fig. 31 Strain Plot for 8 inch Diameter nip and 2.8 pli nip Load

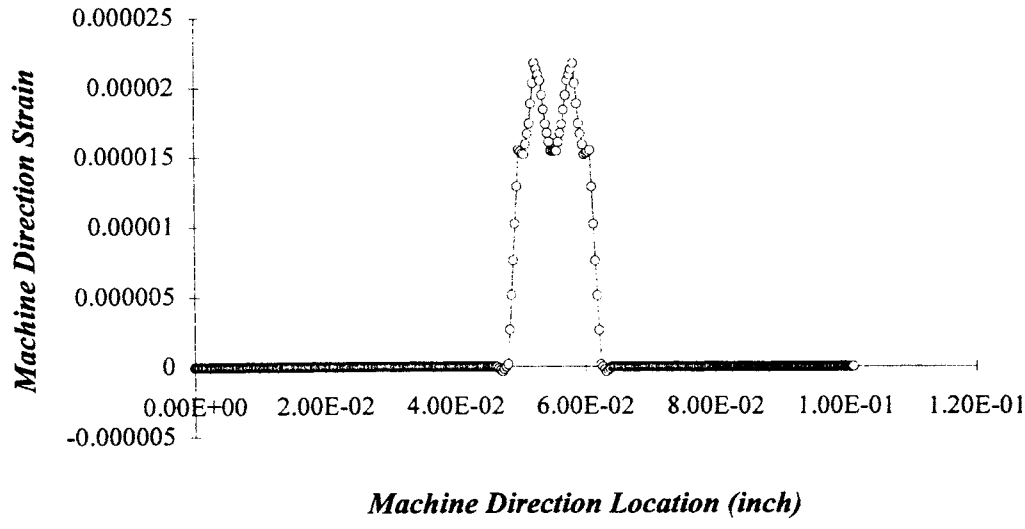

Fig. 32 Strain Plot for 10 inch Diameter nip and 2.8 pli nip Load

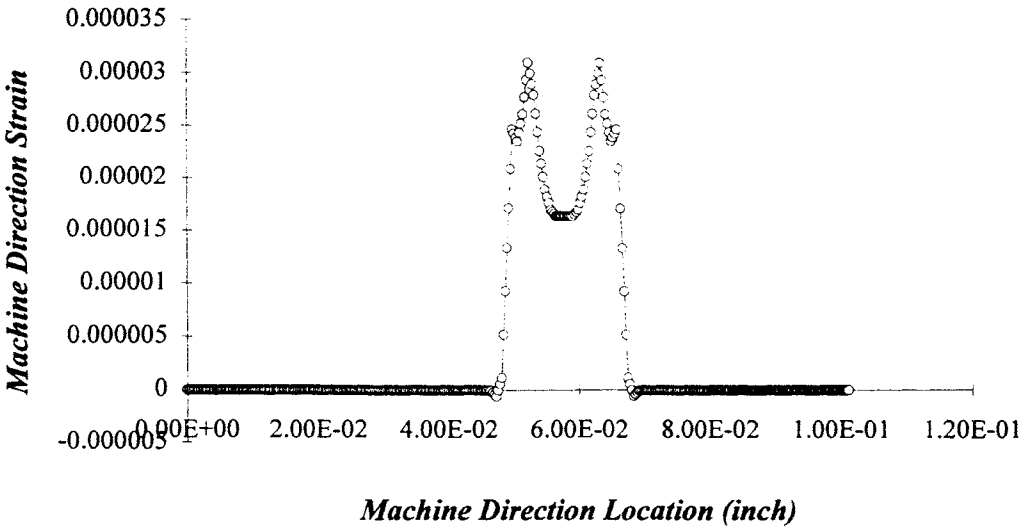

Fig. 33 Strain Plot for 8 inch Diameter nip and 8.26 pli nip Load

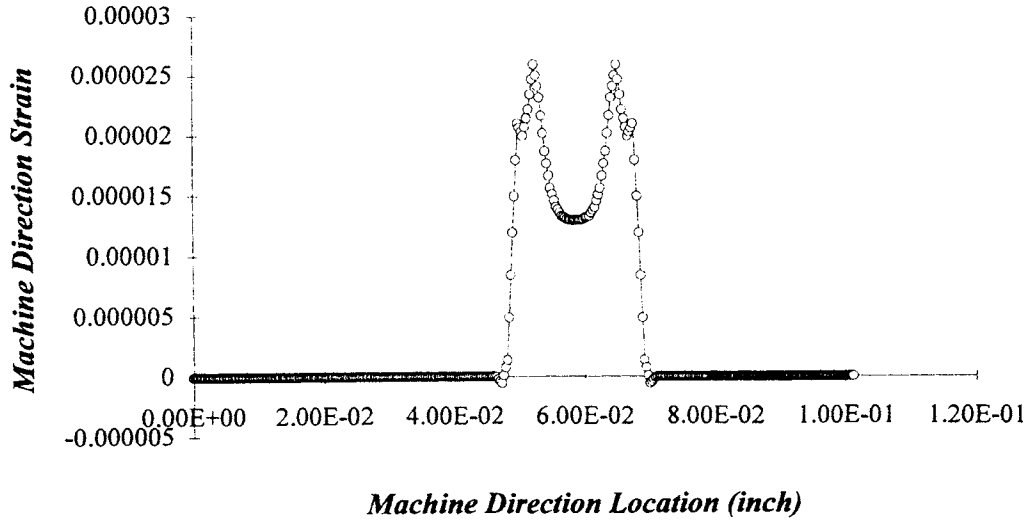

Fig. 34 Strain Plot for 10 inch nip and 8.26 pli nip Load

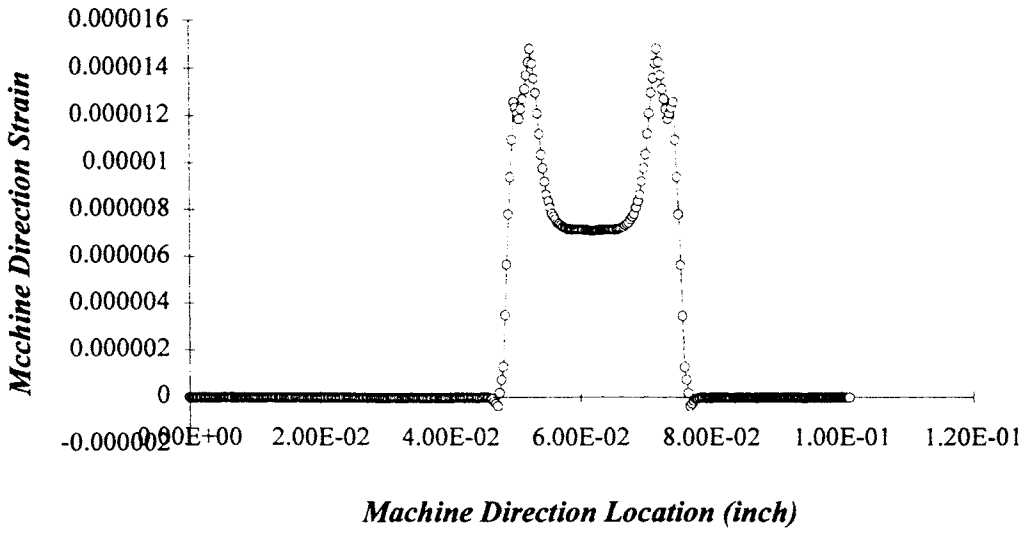

Fig. 35 Strain Plot for 20 inch Diameter nip and 8.26 pli nip Load

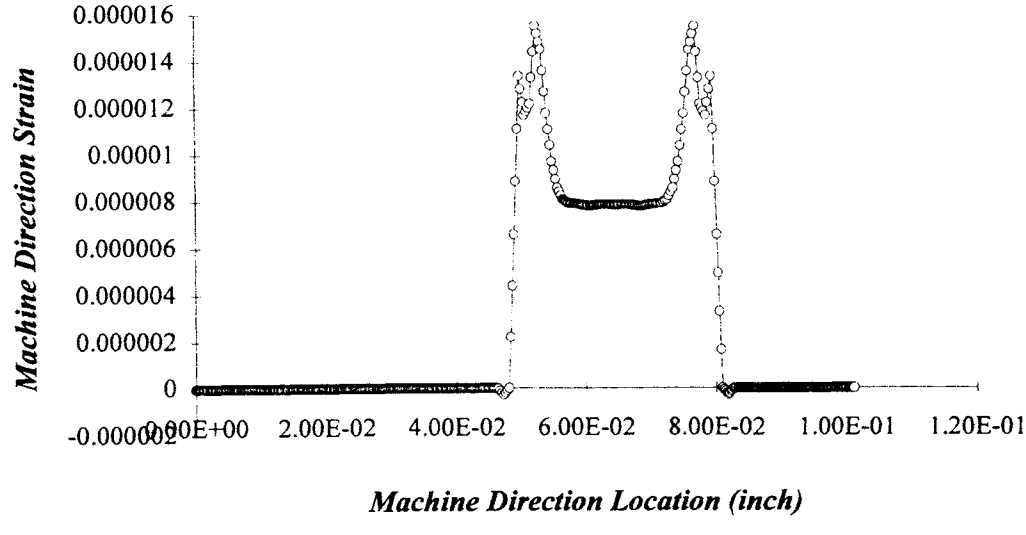

Fig. 36 Strain Plot for 20 inch Diameter nip and 11.77 pli nip Load

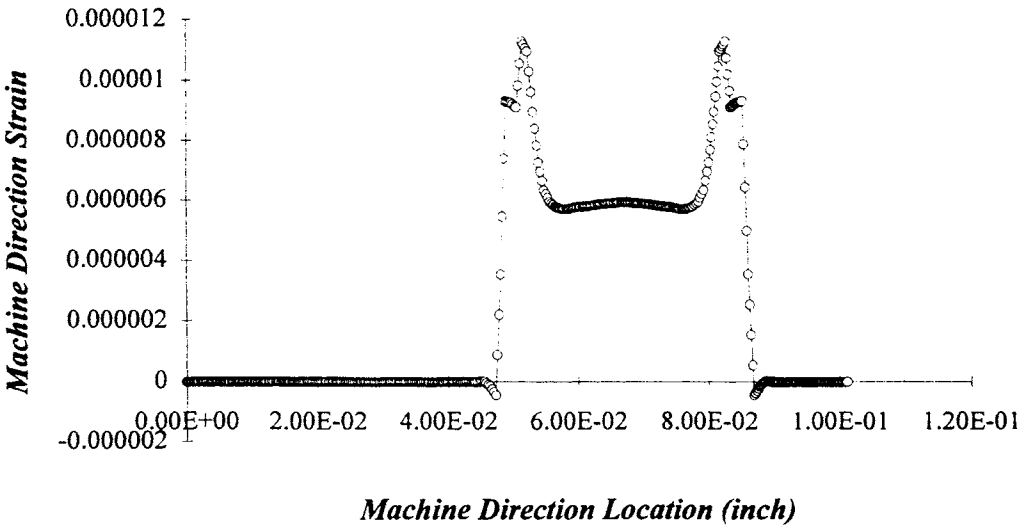

Fig. 37 Strain Plot for 30 inch Diameter nip and 11.77 pli nip Load

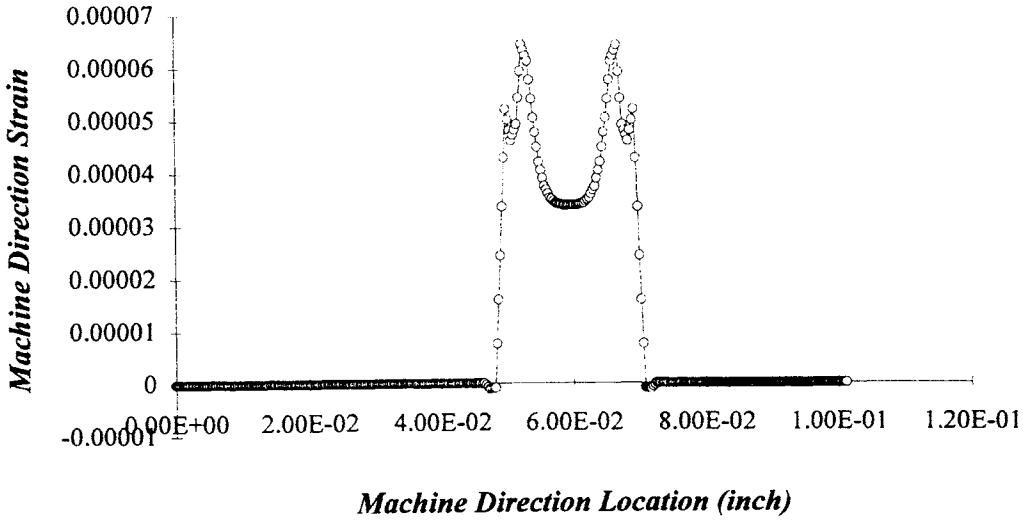

Fig. 38 Strain Plot for 4 inch Diameter nip and 24 pli nip Load

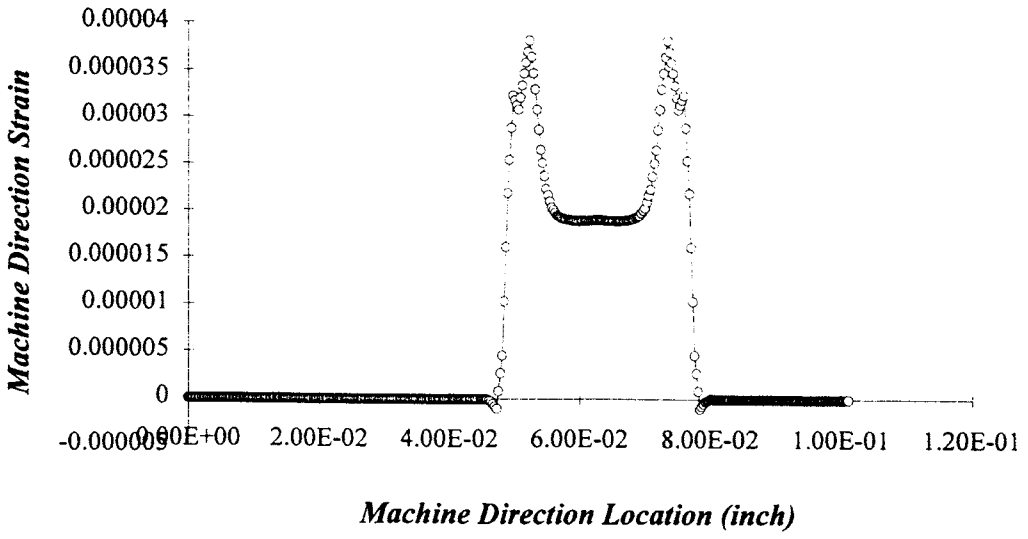

Fig. 39 Strain Plot for 8 inch Diameter nip and 24 pli nip Load

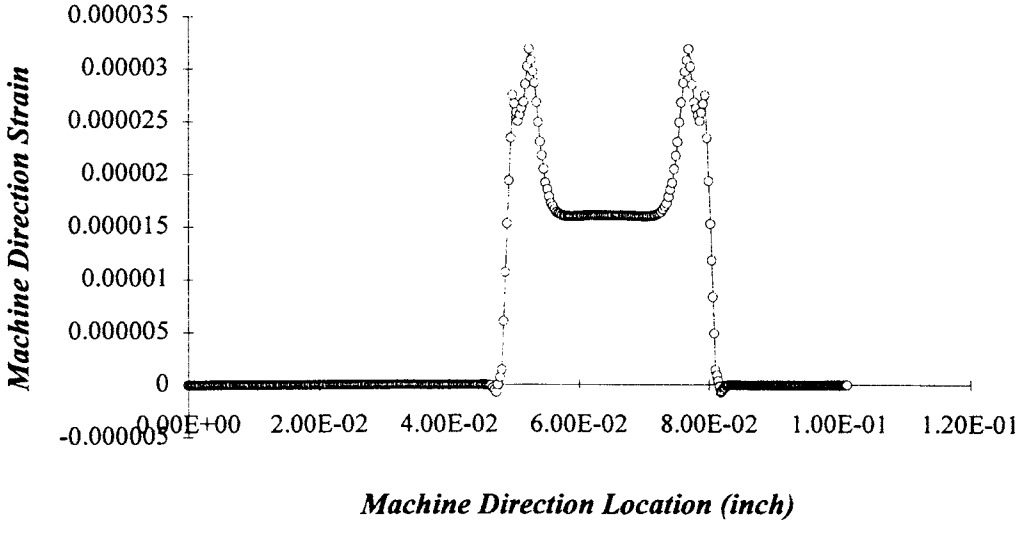

Fig. 40 Strain Plot for 10 inch Diameter nip and 24 pli nip Load

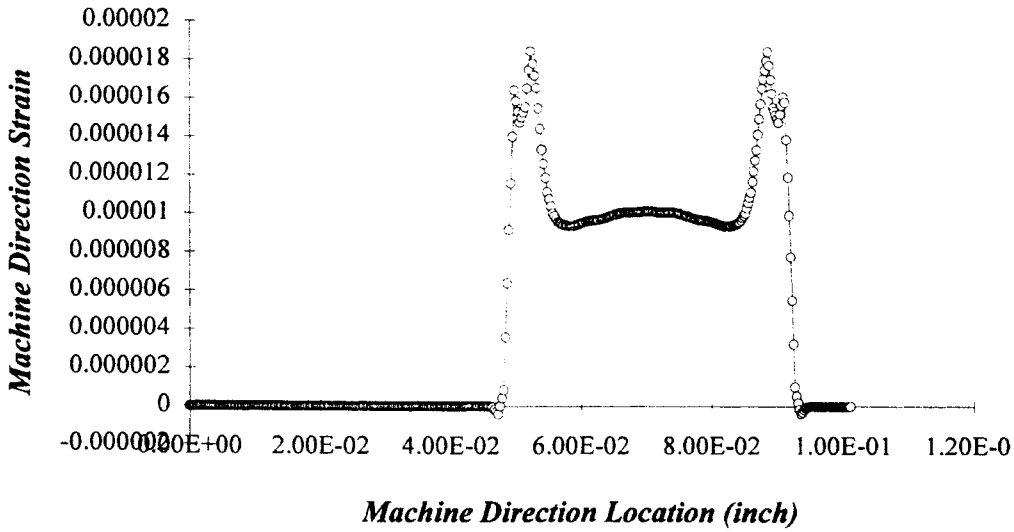

Fig. 41 Strain Plot for 20 inch Diameter nip and 24 pli nip Load

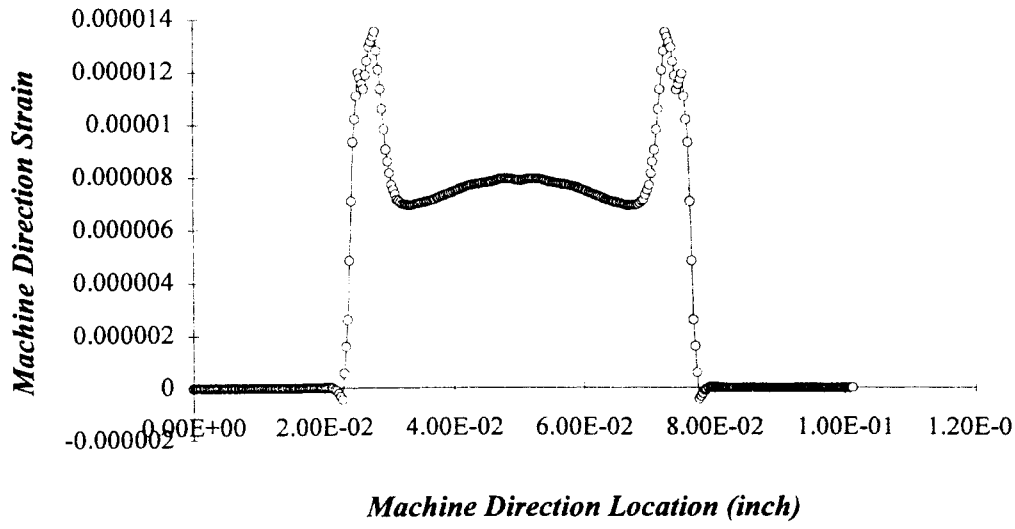

Fig. 42 Strain Plot for 30 inch Diameter nip and 24 pli nip Load

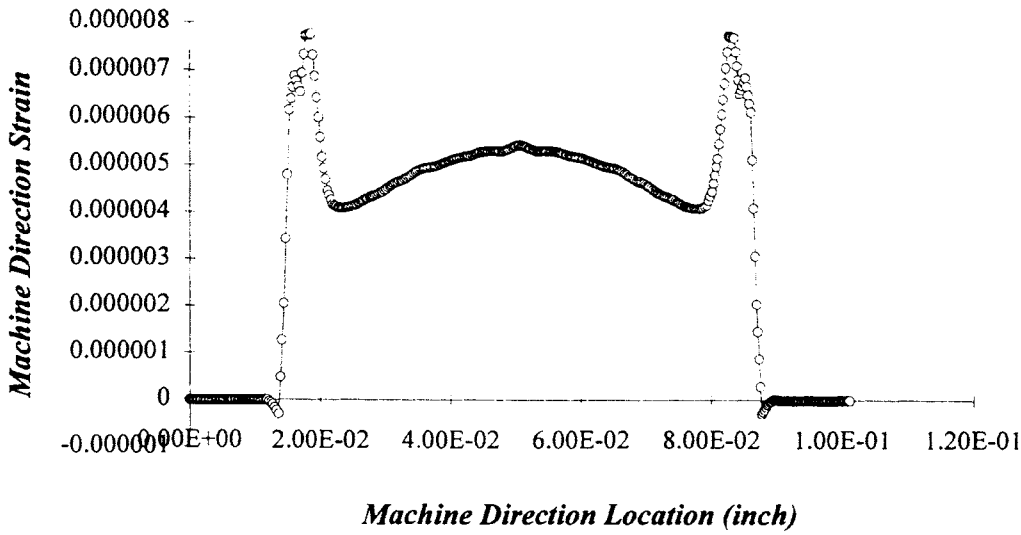

Fig. 43 Strain Plot for 60 inch Diameter nip and 24 pli nip Load

The deformation contribution (C) for 1 inch displacement of nip roller for each of the analysis performed is presented in Table III. The strain in the web for any nip displacement can by evaluated by plugging this value of C in equation {2}.

nip Load (pli)	nip Diameter (inch)	*c*
2.8	8	3.00E-04
	10	2.60E-04
8.26	8	4.56E-04
	10	4.23E-04
	20	3.40E-04
11.77	20	3.65E-04
	30	3.03E-04
24	4	11.34E-04
	8	8.34E-04
	10	7.52E-04
	20	5.81E-04
	30	5.19E-04
	60	4.34E-04

Table III Finite element analysis results

From equation {2}, the web strain approaches a constant value for large nip rolling displacements. Earlier study [2] has shown that although a constant value is appropriate, the nip induced stress cannot exceed the saturation value predicted by $\mu * P / h$. Thus equation {2} can be used for cases in which the saturated value of nip induced strain has not been achieved. It may be noted that the nip induced stress is calculated by multiplying the web strain by Young's modulus as the stress in the web is unidirectional after the passage of the nip.

CHAPTER VI

DISCUSSION

The results obtained from experimental and finite element analysis are presented in fig. 44 through fig. 53 for comparison and discussion.

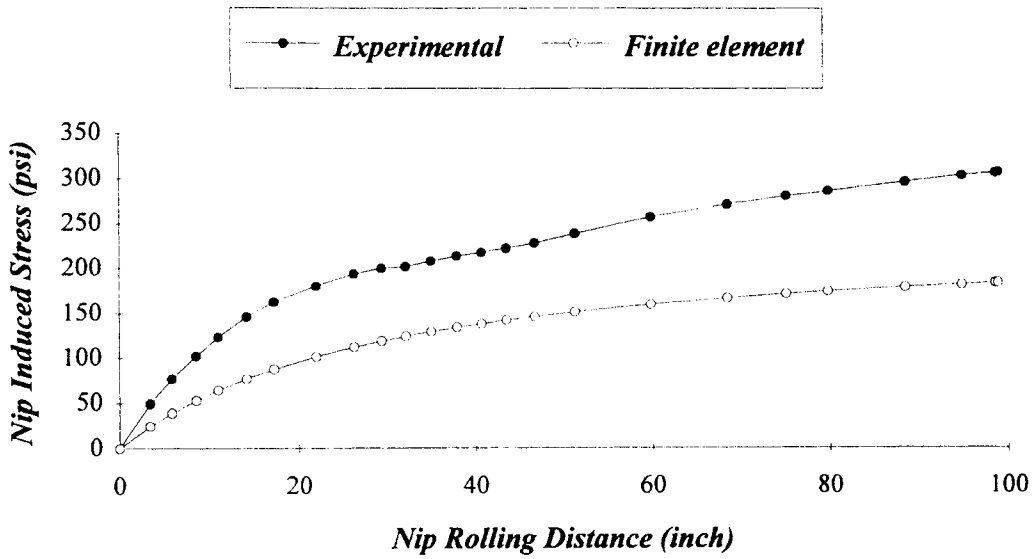

Fig. 44 Comparison of experimental and finite element analysis results for 8 inch diameter nip and 2.8 pli Nip load

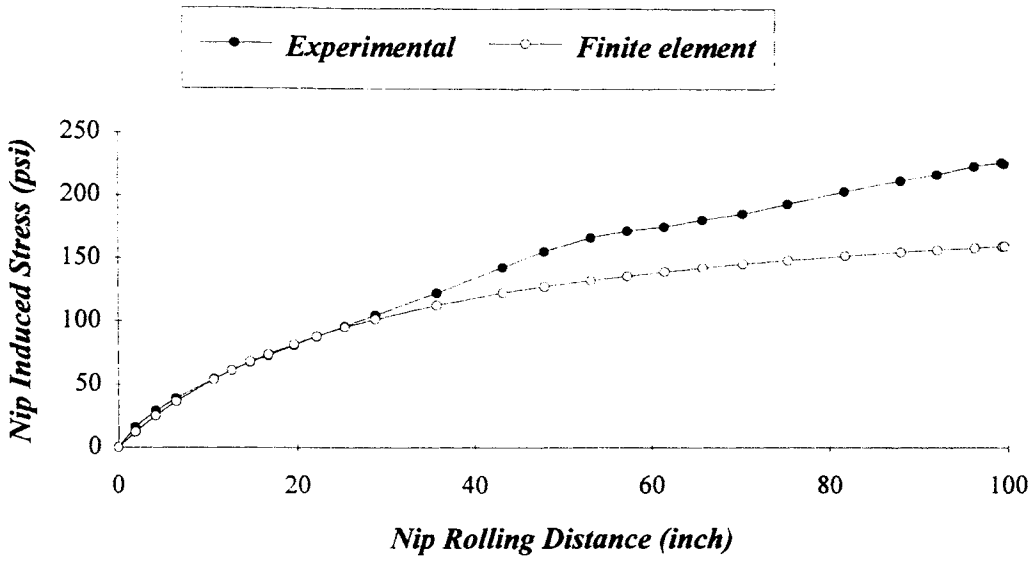

Fig. 45 Comparison of experimental and finite element analysis results for 10 inch diameter nip and 2.8 pli Nip load

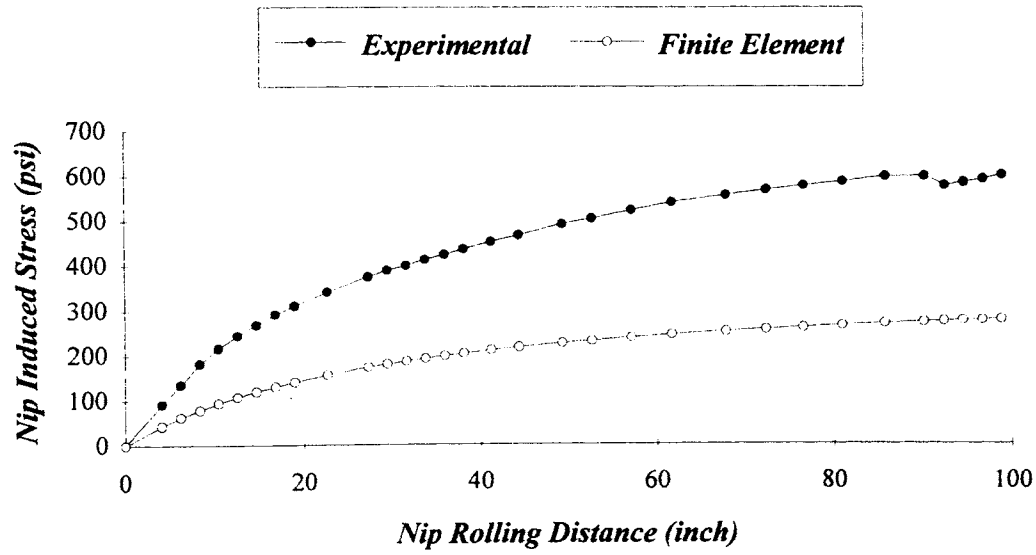

Fig. 46 Comparison of experimental and finite element analysis results for 8 inch diameter nip and 8.26 pli Nip load

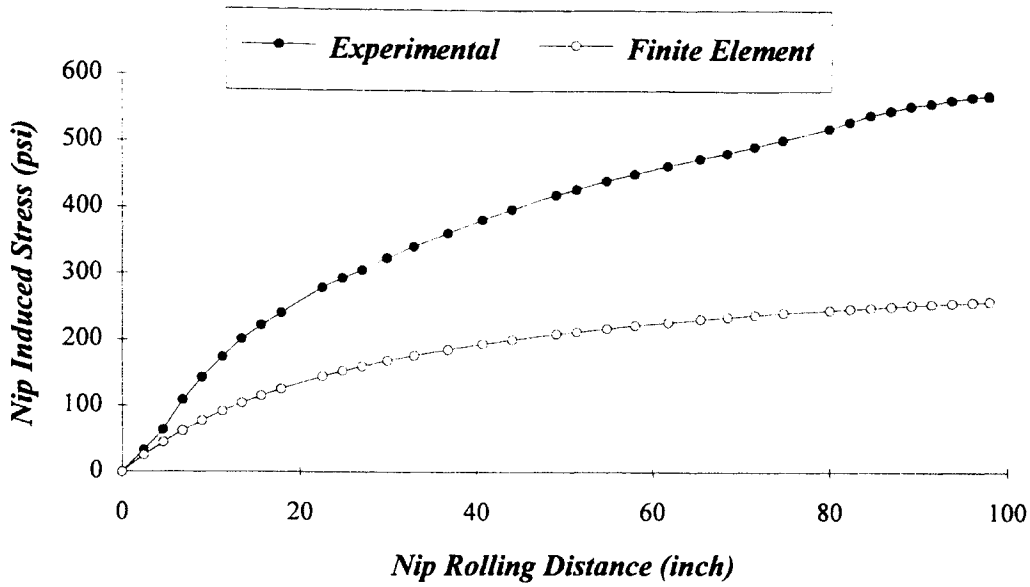

Fig. 47 Comparison of experimental and finite element analysis results for 10 inch diameter nip and 8.26 pli Nip load

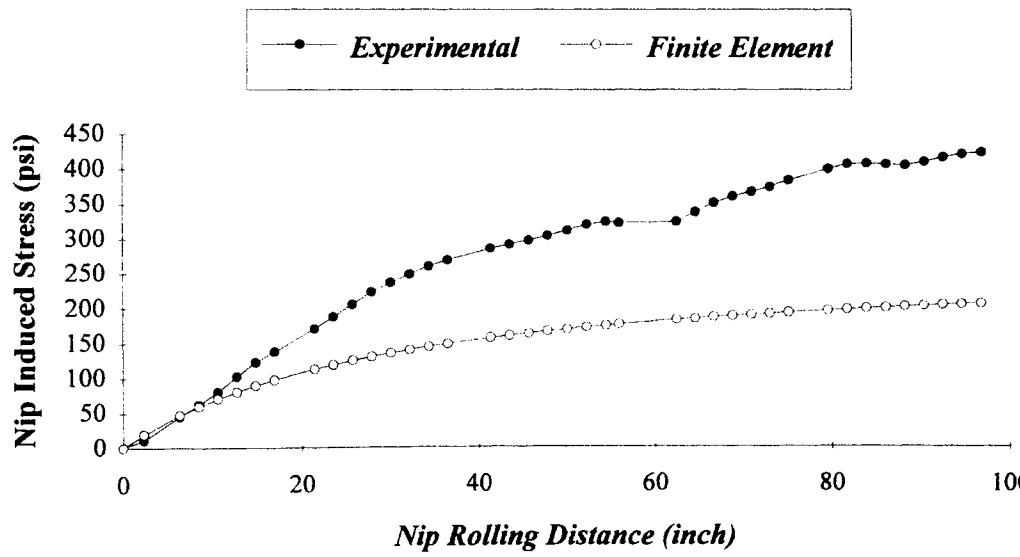

Fig. 48 Comparison of experimental and finite element analysis results for 20 inch diameter nip and 8.26 pli Nip load

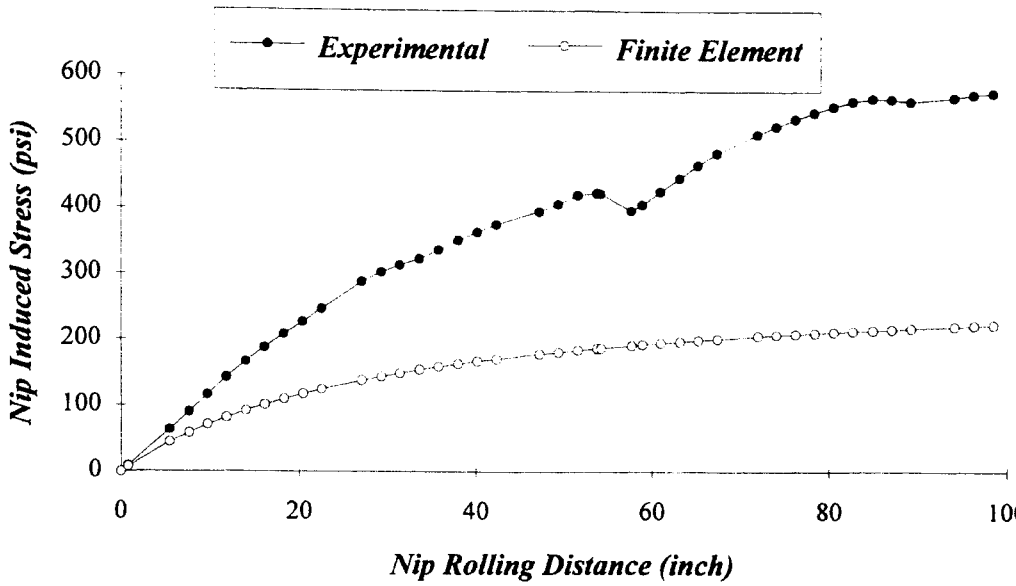

Fig. 49 Comparison of experimental and finite element analysis results for 20 inch diameter nip and 11.77 pli Nip load

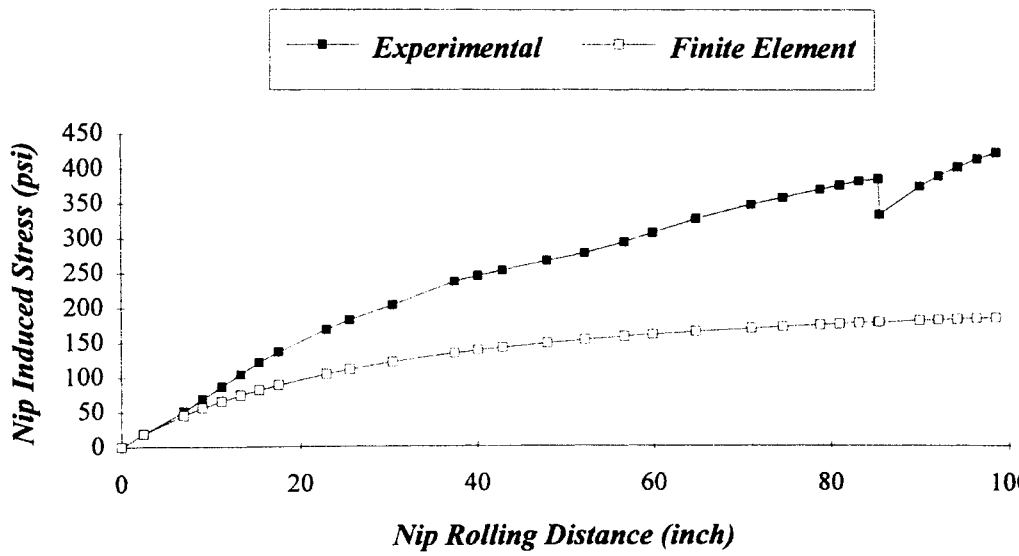

Fig. 50 Comparison of experimental and finite element analysis results for 30 inch diameter nip and 11.77 pli Nip load

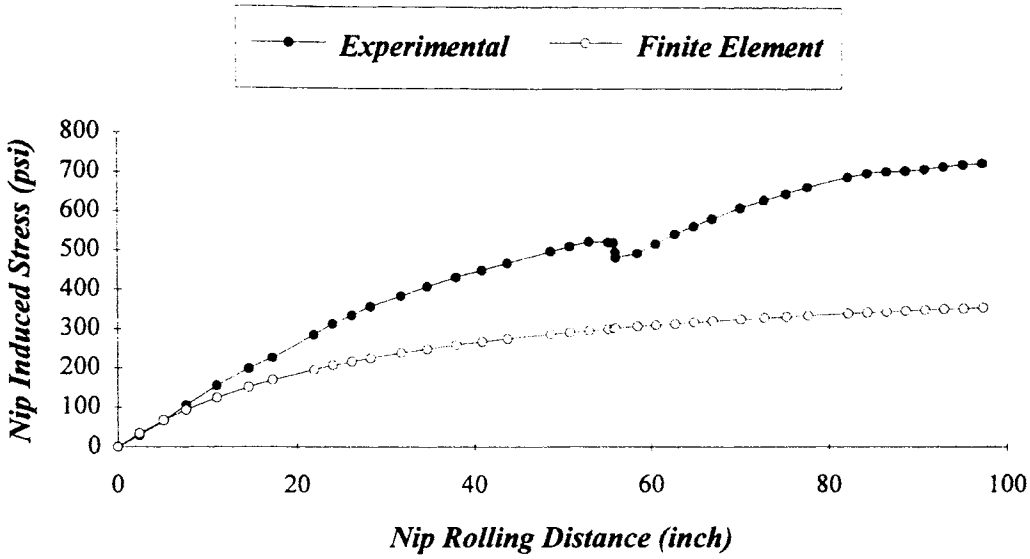

Fig. 51 Comparison of experimental and finite element analysis results for 20 inch diameter nip and 24 pli Nip load

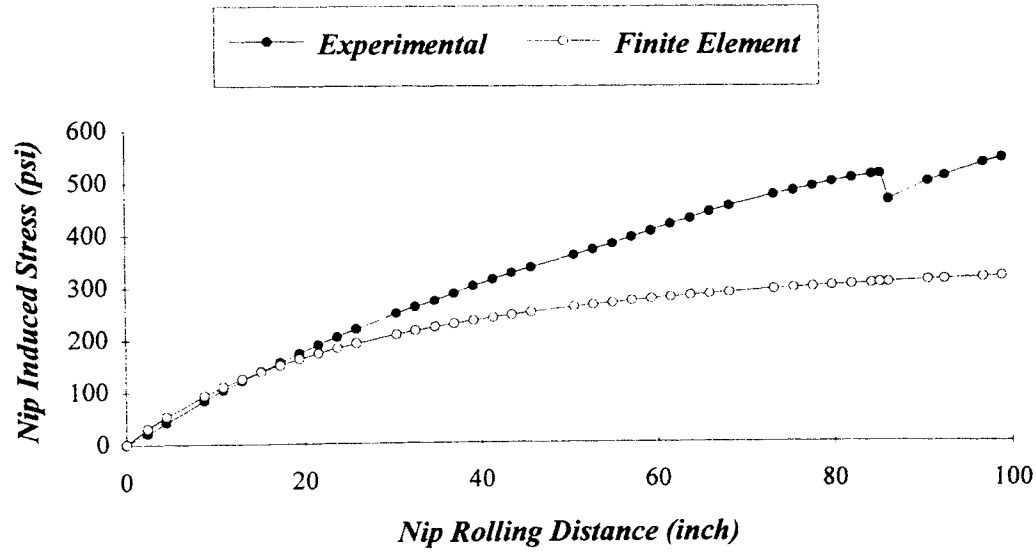

Fig. 52 Comparison of experimental and finite element analysis results for 30 inch diameter nip and 24 pli Nip load

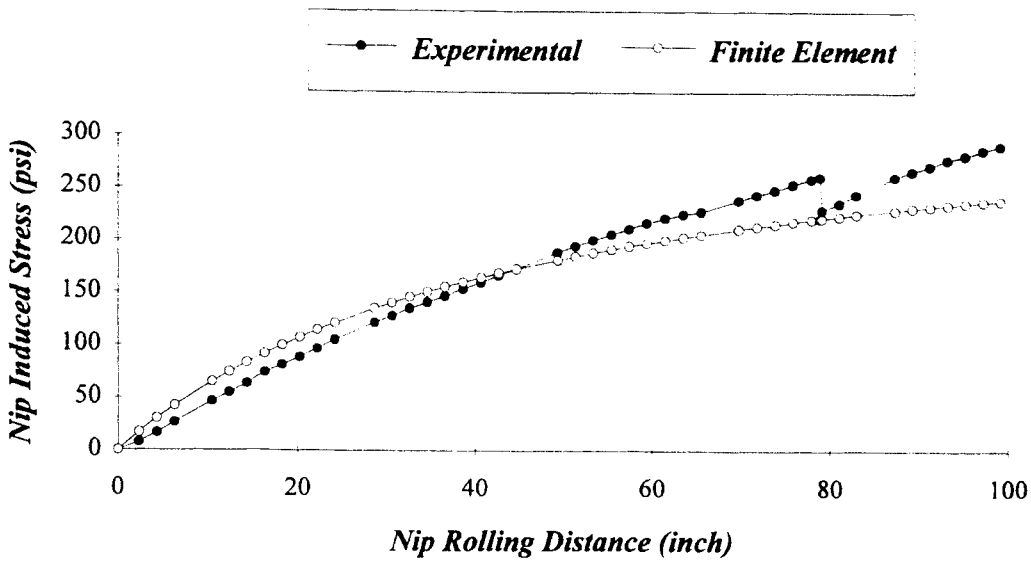

Fig. 53 Comparison of experimental and finite element analysis results for 60 inch diameter nip and 24 pli Nip load

It may be observed form the above figures that the finite element analysis predicted a lower nip induced stress compared to the experimental results. This may be attributed to the fact that the finite element analysis was carried out on a single layer of web, whereas in experimental studies, multiple layer of webs were used. It may also be observed from the results that for a given nip load, the saturated value of nip induced stress decreases as the nip diameter is increased.

Table IV shows a comparison of the saturated values of the nip induced stress that resulted from the experimental & finite element analysis along with the predicted value of $\mu * P / h$.

Nip Load (pli)	Nip Diameter (inch)	Experiment Results (psi)	Finite Element (psi)	$\mu * P / h$ (psi)
2.8	8	362	240	414
	10	315	208	
8.26	8	750	365	1223
	10	679	339	
	20	563	272	
11.77	20	710	292	1744
	30	635	243	
24	4		907	3555
	8		667	
	10		602	
	20	979	465	
	30	808	417	
	60	582	347	

Table IV. Comparison of Nip Induced Stress

It may be noted that in all the cases, the saturated value of nip induced stress is well below the value predicted by $\mu * P / h$. It may also be observed from the table that the saturated value of nip induced stress decreases as the nip diameter increases for the same nip load. Fig. 54a shows a comparison of estimated nip induced stress for different nip diameters for 24 pli nip load. From figure 54a. it can be seen that increase of nip diameter helps to reduce the nip induced stress to a certain extent. But, increasing the nip diameter beyond 30 inch has not resulted in appreciable reduction in nip induced stress.

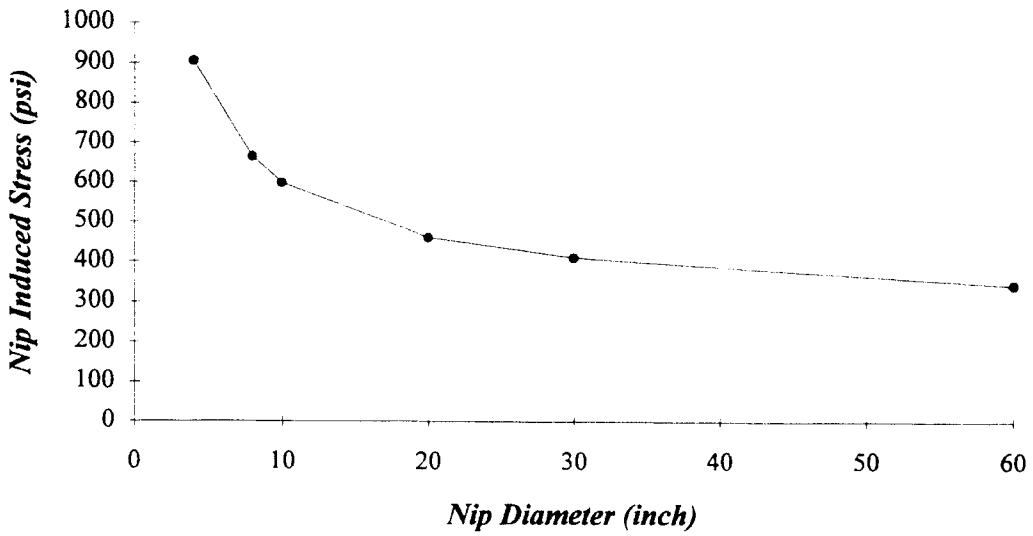

Fig. 54a Comparison of estimated nip induced stress with 24 pli Nip Load for different Nip Diameters

This was the observation made by Frye [1] (fig. 54b) in his experimental studies on winding methods. Even he says "there seems to be a limit where any increase in drum diameter (above 30-34 inch) produces no further improvement in the reduction of wound-in tension". Hence, it can be concluded that increasing the nip diameter beyond a certain level will not help to reduce the nip induced stress.

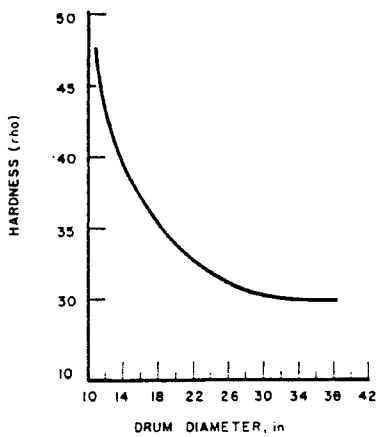

Fig. 54b Effect of nip diameter on roll hardness

CHAPTER VII

CONCLUSIONS AND FUTURE WORK

Conclusions

The results of analysis has proved that the rate of nip induced stress depends on the nip diameter. The nip induced stress increases at a faster rate and saturates quickly for smaller diameter nips compared to large diameter nips, with other winding parameters remaining same. The saturated value of nip induced stress depends on the nip load and the nip diameter, while the rate of nip induced stress is dependent on the nip diameter. Thus, increasing the nip diameter to a certain extent helps to reduce the nip induced stress. It can also be seen from the analysis that increasing the nip diameter beyond 30 inch produces no further improvement in the reduction of nip induced stress. Also, in the case of large diameter nips, the nip induced stress will be $\varepsilon_x * E$ which is below the value predicted by $\mu * P/h$. The value of ε_x can be calculated using equation {2}, in which the constant C determined by finite element methods. For large nip rolling distances,ε_x will approach C. It was observed that the constant C decreases with increased nip diameter.

Hence, it can be concluded that for the cases of large diameter nips, the nip induced stress will not reach the value predicted by $\mu * P/h$ and hence the equation for wound-on-tension will be :

$$WOT = T_w + \varepsilon_x * E \qquad \{11\}$$

where T_w is the web line tension.

Future Work

1. Multiple layers of web needs to be modeled by finite element analysis to accurately simulate the experimental work.
2. A model to accommodate the effect of uneven nip roller profile is required. The nip pressure across the machine width is never uniform and with an uneven profile across the roll, nip induced tension is not uniform.
3. Work has to be undertaken to modify the closed form equation {6} to accomodate thickness of web.

REFERENCES

1. Frye, Kenneth.G, "New winding methods and basic winding parameters "TAPPI Journal, Vol. 68, No. 5, May 1988, pp. 66-72.
2. Good, J.K., Wu, Z., and Fikes, M.W.R., "The Internal Stresses in wound rolls with the presence of a nip roller". Submitted for review to the Journal of Applied mechanics, May 1990.
3. Johnson, K.L., Contact Mechanics, Cambridge University Press, New York, 1989, pp. 312 - 314.
4. Pfeiffer, J.D., "Mechanics of Rolling on Paper webs". TAPPI Journal, Vol. 51, No. 8, August 1968, pp. 77A-85A,.
5. Radzimovsky, E.I., "Stress distribution and strength condition of two rolling cylinders pressed together". Univ. Ill. Engr. Expt. Station, Bulletin 408, 1953, pp. 1-40.
6. Shigley, Joseph.E., and Mitchell, Larry.D., Mechanical Engineering Design, Fourth Edition, McGraw-Hill Book Company, New York, 1983, pp. 340 - 342.
7. Vaidyanathan Nandakumar, "An Investigation of the Nip Induced Tension Mechanism Using Photo elasticity." MS Report, Department of Mechanical and Aerospace Engineering, Oklahoma State University, May 1989.
8. Wu, Z., "An Investigation of the Effect of Nip Mechanics upon Wound Roll Stresses." Ph.D. Thesis, Department of Mechanical and Aerospace Engineering, Oklahoma State University, July 1990.

APPENDIX

Finite element (ANSYS) code for Analysis

```
/PREP7
/title, single layer with 8 inch diameter nip roll & 27 lbf Load.
KYPOST,0
KAY,6,1
ET,1,42,0,1,2,,0,0   ! 2-D 4-node isoparameteic solid, with plane strain
ET,2,1,0             ! 2-D spar element
ET,3,26,1            ! 2-D contact surface element
! Real constants and material properties
R,1,0
MP,EX,1,800000
MP,NUXY,1,.01
R,2,0.000153409,0
MP,EX,2,800000
R,3,1E7,,,1E7
MP,MU,3,.25
! Model
N,1,0,0
N,121,0.10125,0
FILL,1,121
NGEN,11,121,ALL,,,,0.00016875
N,1332,-30.0,0
N,1342,-30.0,0.0016875
FILL,1332,1342
N,1343,0,0
N,1344,0.10125,0
TYPE,1
REAL,1
E,1,2,123,122
EGEN,120,1,1
E,122,123,244,243
EGEN,120,1,121
E,243,244,365,364
EGEN,120,1,241
E,364,365,486,485
EGEN,120,1,361
E,485,486,607,606
EGEN,120,1,481
E,606,607,728,727
EGEN,120,1,601
E,727,728,849,848
```

```
EGEN,120,1,721
E,848,849,970,969
EGEN,120,1,841
E,969,970,1091,1090
EGEN,120,1,961
E,1090,1091,1212,1211
EGEN,120,1,1081
TYPE,2
REAL,2
E,1332,1
E,1333,122
E,1334,243
E,1335,364
E,1336,485
E,1337,606
E,1338,727
E,1339,848
E,1340,969
E,1341,1090
E,1342,1211
TYPE,3
REAL,3
E,1,1343,1344
RP121,1
! Loads and boundary conditions
D,1343,ALL,0.0
D,1344,ALL,0.0
D,1332,ALL,0.0,,1342,1
ITER,-5
*CREATE, LOAD1
EP,1140,3,(ARG1)
LWRITE
*END
*USE,LOAD1,0
RP12,,(88.4/12)
*CREATE,LOAD2
EP,1140,3,(ARG2)
EP,1141,3,(0.348*ARG2)
LWRITE
*END
*USE,LOAD2,0
RP12,,(254/12)
*CREATE,LOAD3
EP,1140,3,(ARG3)
EP,1141,3,(0.768*ARG3)
```

```
EP,1142,3,(0.267*ARG3)
LWRITE
*END
*USE,LOAD3,0
RP12,,(330.7/12)
*CREATE,LOAD4
EP,1140,3,ARG4
EP,1141,3,(0.88*ARG4)
EP,1142,3,(0.68*ARG4)
EP,1143,3,(0.24*ARG4)
LWRITE
*END
*USE,LOAD4,0
RP12,,(375.1/12)
*CREATE,LOAD5
EP,1140,3,ARG5
EP,1141,3,(0.94*ARG5)
EP,1142,3,(0.83*ARG5)
EP,1143,3,(0.64*ARG5)
EP,1144,3,(0.22*ARG5)
LWRITE
*END
*USE,LOAD5,0
RP12,,(399.6/12)
*CREATE,LOAD6
EP,1140,3,ARG6
EP,1141,3,(0.98*ARG6)
EP,1142,3,(0.92*ARG6)
EP,1143,3,(0.81*ARG6)
EP,1144,3,(0.62*ARG6)
EP,1145,3,(0.22*ARG6)
LWRITE
*END
*USE,LOAD6,0
RP12,,(407.3/12)
*CREATE,LOAD7
EP,1140,3,(0.98*ARG7)
EP,1141,3,(ARG7)
EP,1142,3,(0.98*ARG7)
EP,1143,3,(0.92*ARG7)
EP,1144,3,(0.81*ARG7)
EP,1145,3,(0.623*ARG7)
EP,1146,3,(0.22*ARG7)
LWRITE
*END
```

```
*USE,LOAD7,0
RP12,,(407.3/12)
*CREATE,LOAD8
EP,1140,3,(0.921*ARG8)
EP,1141,3,(0.981*ARG8)
EP,1142,3,(ARG8)
EP,1143,3,(0.981*ARG8)
EP,1144,3,(0.921*ARG8)
EP,1145,3,(0.812*ARG8)
EP,1146,3,(0.624*ARG8)
EP,1147,3,(0.22*ARG8)
LWRITE
*END
*USE,LOAD8,0
RP12,,(407.3/12)
*CREATE,LOAD9
EP,1140,3,(0.812*ARG9)
EP,1141,3,(0.921*ARG9)
EP,1142,3,(0.981*ARG9)
EP,1143,3,(ARG9)
EP,1144,3,(0.981*ARG9)
EP,1145,3,(0.921*ARG9)
EP,1146,3,(0.812*ARG9)
EP,1147,3,(0.624*ARG9)
EP,1148,3,(0.22*ARG9)
LWRITE
*END
*USE,LOAD9,0
RP12,,(407.3/12)
*CREATE,LOAD10
EP,1140,3,(0.624*ARG10)
EP,1141,3,(0.812*ARG10)
EP,1142,3,(0.921*ARG10)
EP,1143,3,(0.981*ARG10)
EP,1144,3,(ARG10)
EP,1145,3,(0.981*ARG10)
EP,1146,3,(0.921*ARG10)
EP,1147,3,(0.812*ARG10)
EP,1148,3,(0.624*ARG10)
EP,1149,3,(0.22*ARG10)
LWRITE
*END
*USE,LOAD10,0
RP12,,(407.3/12)
*CREATE,LOAD11
```

```
EP,1140,3,(0.22*ARG11)
EP,1141,3,(0.624**ARG11)
EP,1142,3,(0.812*ARG11)
EP,1143,3,(0.921*ARG11)
EP,1144,3,(0.981*ARG11)
EP,1145,3,(ARG11)
EP,1146,3,(0.981*ARG11)
EP,1147,3,(0.921*ARG11)
EP,1148,3,(0.812*ARG11)
EP,1149,3,(0.624*ARG11)
EP,1150,3,(0.22*ARG11)
LWRITE
*END
*USE,LOAD11,0
RP12,,(407.3/12)
*CREATE,LOAD12
EP,1140,3,0
EP,1141,3,(0.22*ARG12)
EP,1142,3,(0.624*ARG12)
EP,1143,3,(0.812*ARG12)
EP,1144,3,(0.921*ARG12)
EP,1145,3,(0.981*ARG12)
EP,1146,3,(ARG12)
EP,1147,3,(0.981*ARG12)
EP,1148,3,(0.921*ARG12)
EP,1149,3,(0.812*ARG12)
EP,1150,3,(0.624*ARG12)
EP,1151,3,(0.22*ARG12)
LWRITE
*END
*USE,LOAD12,0
RP12,,(407.3/12)
*CREATE,LOAD13
EP,1141,3,0
EP,1142,3,(0.22*ARG13)
EP,1143,3,(0.624*ARG13)
EP,1144,3,(0.812*ARG13)
EP,1145,3,(0.921*ARG13)
EP,1146,3,(0.981*ARG13)
EP,1147,3,(ARG13)
EP,1148,3,(0.981*ARG13
EP,1149,3,(0.921*ARG13)
EP,1150,3,(0.812*ARG13)
EP,1151,3,(0.624*ARG13)
EP,1152,3,(0.22*ARG13)
```

```
LWRITE
*END
*USE,LOAD13,
RP12,,(407.3/12)
AFWRITE,,1,0
FINISH
```

VITA

Mohan Prabhakar

Candidate for the Degree of

Master of Science

Thesis : STUDY OF THE EFFECT OF NIP DIAMETER ON THE RATE OF NIP INDUCED TENSION.

Major Field: Mechanical Engineering.

Biographical:

Personal Data: Born in Mysore, India, On December 10, 1961, the son of Dr.S.V.Prabhakar and Sunanda.

Education: Graduated from M.M.Junior College, Mysore, India, in June 1978; received Bachelor of Engineering in mechanical Engineering degree in 1983 from Mysore University, India; Completed the requirements for the Master of Science degree at Oklahoma State University in May 1994.

Professional Experience: Lecturer, Department of Mechanical Engineering, S.J. College of Engineering, Mysore, India, 1984; Assistant Engineer (Manufacturing), Bharat Electronics, Bangalore, India, 1985-88; Senior Engineer (R&D), Bharat Electronics, India, 1989-92.